Paper to be presented at the 4th Incipient Failure Detection Conference - Predictive Maintenance for the '90's, October 15-17, 1990 in Philadelphia, PA, sponsored by EPRI.

CONF-901058--1

DE90 012595

Use of Motor Current Signature Analysis at the EPRI M&D Center

H. D. Haynes
R. C. Kryter
B. K. Stewart

Oak Ridge National Laboratory*
Advanced Diagnostic Engineering R&D Center
Oak Ridge, Tennessee

*Operated by Martin Marietta Energy Systems, Inc. for U.S. Department of Energy under contract DE-AC05-84OR21400

Use of Motor Current Signature Analysis at the EPRI M&D Center

H. D. Haynes
R. C. Kryter
B. K. Stewart

Oak Ridge National Laboratory*
Advanced Diagnostic Engineering R&D Center
Oak Ridge, Tennessee

ABSTRACT

Motor current signature analysis (MCSA), a machinery monitoring technology developed by the Oak Ridge National Laboratory (ORNL), has been used to monitor a variety of electric-motor-driven devices at the Philadelphia Electric Company's Eddystone Generating Station as part of a program conducted by the EPRI Monitoring and Diagnostics Center. The purpose of this project is to demonstrate the ability of MCSA to monitor the occurrence of degradation in aging power plant equipment. An important aspect of the work has been the development and demonstration of an on-line, automated motor current data acquisition system for monitoring the performance of eight motor-operated valves (MOVs) located in the Unit 2 turbine steam extraction system.

Improvements continue to be made in the on-line monitoring system, including development of an automated data analysis program that significantly reduces the time required to extract diagnostic information from the MOV motor current signatures.

Using portable MCSA equipment, motor current data were acquired for additional MOVs, pumps, fans, compressors, and mills. These tests have provided important baseline signatures against which subsequent test data may be compared.

This paper provides descriptions of the tested equipment, the MCSA techniques employed, samples of test data acquired from both the on-line and portable data acquisition systems, and plans for future work in this ongoing effort.

*Operated by Martin Marietta Energy Systems, Inc. for U.S. Department of Energy under contract DE-AC05-84OR21400

1. INTRODUCTION

1.1 Background

In 1989 the Oak Ridge National Laboratory (ORNL) established an Advanced Diagnostic Engineering Research and Development Center (ADEC) to establish a position in the relatively new field of diagnostic engineering. ADEC is an organized diagnostics research program that brings together experts in many scientific disciplines to develop and apply new and advanced diagnostic technologies to real-world problems, especially those in the power generation industry.

A promising new machinery monitoring technology, motor current signature analysis (MCSA), is the focus of several ADEC tasks. MCSA is based on the principle that a conventional electric motor (ac or dc) driving a mechanical load acts as an efficient and permanently available transducer, detecting small time-dependent motor load variations generated anywhere within the mechanical system and converting them into electric-current noise signals that flow along the power cable. These signals bear information concerning the "health" of both the motor and the driven device.

Initially, MCSA technology was developed by ORNL as a means for determining the effects of aging and service wear on motor-operated valves (MOVs), and research has demonstrated the sensitivity and selectivity of several MOV motor current signature features to purposely implanted defects and simulated degradation [1, 2]. However, MCSA is now recognized to be applicable to a much broader range of machinery than MOVs. An important objective of ADEC is therefore to demonstrate advanced monitoring applications utilizing MCSA on such additional equipment as pumps, fans, compressors, and mills.

The EPRI Monitoring and Diagnostics (M&D) Center at the Philadelphia Electric Company's Eddystone Generating Station has provided ORNL/ADEC a unique opportunity to apply, on a relatively long-term basis, MCSA technology as an on-line diagnostic monitoring technique. During the period October 1989 through January 1990, over 1200 MOV actuations have been recorded and analyzed, and motor current signatures from a limited number of pumps, fans, compressors, and mills have also been acquired and analyzed [3, 4], as detailed in Sect. 1.3. These tests have provided important baseline performance characteristics against which subsequent test data may be compared.

1.2 Work Objectives

The ORNL/ADEC work at Eddystone has the following major objectives:

1. Demonstrate the workability of an automated MOV data acquisition system in a real plant environment,

2. Obtain long-term performance data from service-aged MOVs,

3. Demonstrate a correspondence between MOV parameter trends and performance problems or other signs of degradation, and

4. Demonstrate the usefulness of MCSA for monitoring motor-driven equipment other than MOVs.

Owing to the relatively short length of time that the MCSA system has been in service at Eddystone, none of the work objectives can be said to be completed at the time of this writing. However, it is our expectation that as time and service stressors take their toll, evidences of degradation will appear and all the objectives will eventually be satisfied.

1.3 Equipment Tested

A list of the motor-driven devices at the Eddystone power plant to which motor current data acquisitions and analyses have been applied are shown in Table 1.

Table 1. Motor-Driven Equipment at the Eddystone Power Plant Tested October 1989 through April 1990 Using MCSA

Device	Number of Units Tested	Number of Tests Performed
Motor-Operated Valves	16	> 1200
Induced-Draft Fans	2	2
Boiler Feed Pumps	4	5
Mills	2	2
Air Compressors	2	2
Condensate Feed Pumps	1	1
Test Rig with Purposely Faulted Drive Motor	1	4

The following sections of this paper provide information on these devices and the results obtained from their tests.

2. TEST METHODOLOGIES AND RESULTS

Before discussing the results obtained to date, a description of the on-line motor current signature monitoring system is presented below.

2.1 ORNL MOV On-Line Monitoring System Description

2.1.1 Data acquisition system. The ORNL-developed system is shown schematically in Fig. 1. MOV motor current signals are acquired non-intrusively by 400:1 ratio toroidal current transformers, each placed on a motor lead accessible near the motor control center serving the MOVs. The reduced ac current signals supplied by the secondary sides of the current transformers are transmitted via shielded twisted-pair cables to a data acquisition room, where they are connected to signal processing equipment developed specifically for this application. Here each individual cable is terminated by a 10-Ω load resistor and the resulting voltages are input to a summing amplifier, the output of which receives additional signal conditioning (amplification, demodulation, and filtration).

The use of the above voltage summing scheme is predicated on the assumption that only one MOV will be actuated at a time. If more than one MOV is actuated simultaneously, the summed signal will contain elements (usually inseparable) of all energized MOVs, thereby rendering the signal useless for analysis.

During an MOV actuation, the signal processing equipment provides two simultaneous analog outputs, the first optimized for time-domain (waveform) analysis and the other for frequency-domain (spectral) analysis. In addition to the two analog signals, a digital signal is also generated that provides the identity of the MOV being actuated. The three signals are carried by cables to a nearby data display room where they are monitored continuously by a computer-based data acquisition system executing custom software written by ORNL.

At present, MOV signature development is a four-step, manually assisted process consisting of data acquisition, data transfer, database construction, and data analysis. System improvements are being made to streamline this process so that all functions can be carried out at Eddystone by M&D Center personnel.

2.1.2 Data processing. Initially all data analyses were done manually, that is, by displaying a selected signature using a commercial data plotting program, categorizing the run (normal or abnormal) by examining the signature for the presence of specific features, and measuring all desired signature parameters via movable cursors (pointers) provided by the plotting program. This method of data analysis required considerable time of a person having MCSA expertise, so to speed up the analysis process an automated feature extraction program was developed. The program, named RESOLVE, has proved capable of distinguishing between normal and abnormal motor current signatures (the latter caused, in part, by operator actuation of more than one valve at a time). RESOLVE can also identify and quantify several types of transient phenomena (e.g., motor startup and trip, or hammerblow within the motor operator) that are present in normal MOV signatures, and determines for each valve actuation the following trendable performance indicators:

- Valve stroke time
- Maximum running current achieved
- Minimum running current achieved
- Average running current
- Peak current values for transients
- Probable stroke direction
  (i.e., open-to-close, or close-to-open)

The accuracy of RESOLVE has been confirmed by thorough comparisons against data sets analyzed manually.

2.2 MOV Test Results

The ORNL MOV on-line motor current signature monitoring system is presently dedicated to eight turbine steam extraction valves in Unit 2, a majority of the monitoring experience acquired by ORNL/ADEC at the Eddystone Generating Station has been in connection with these valves. These MOVs are open during normal plant operation so as to permit steam to flow from various turbine sections for the purpose of heating boiler feedwater. The extracted steam is routed to eight individual feedwater heaters (5A, 5B, 6A, 6B, 7A, 7B, 8A, 8B) through lines equipped with respectively designated block valves. It is imperative that these block valves close in the event of a significant feedwater heater tube leak (to avoid water ingress into the turbine); thus, they are stroked (closed, then reopened) daily to insure operability.

Motor current signature analysis has been performed using the on-line monitoring system on eight steam extraction valves in Unit 2. Using manual data acquisition equipment, comparable analyses have been performed on eight similar valves in Unit 3. The Unit 2 valves utilize Limitorque motor operators having motors manufactured by Peerless or Reliance and rated for 3-phase, 60 Hz, 208-V power; the Unit 3 valves are similar, but powered by 440 V. All motors have a nominal running speed of 1750 rpm.

Data have been analyzed in both time and frequency domains and are discussed in the following sections.

2.2.1 Time Domain Results

2.2.1.1 Incomplete valve closure. Upon viewing the time-domain signatures, an immediate, observation of considerable importance to the plant is that none of the eight Unit 2 valves shows any degree of motor current rise at the end of the open-to-close stroke that would be indicative of the valve obturator encountering its seat (see Fig. 2, for example). Such lack of complete closure seems contradictory to the functional requirement for these valves, namely, the prevention of water backflow into the turbine in the event of a boiler feedwater heater tube rupture. After disclosing this observation to Eddystone plant personnel, we were informed that the mechanism used for tripping the steam extraction valve motors is the motor operator limit switch, rather than the torque switch, as is customarily employed to ensure valve closure. As a result of this finding, use of the torque switch is being considered by plant operations personnel. In contrast to the Unit

2 MOVs, the motor current signatures from Unit 3 valves showed signs of full closure but varying seating margins, as shown in Fig. 3.

2.2.1.2 Operator hammerblow and valve differential pressure. Since the Unit 2 steam extraction valves do not close hard against their seats, gate seating/unseating transients would not be expected. However, two other transient types have been observed. These additional transients, which occur during the open-to-close strokes of valves 7A, 8A, and 8B, seem to be attributable to motor operator hammerblow and valve differential pressure loads.

A typical open-to-close hammerblow transient is shown in Fig. 4 for Unit 2 extraction valve 7A. The transient is seen to begin ~0.64 s after the motor is energized and constitutes a momentary rise in current of ~0.5 A. This current rise reflects an additional motor torque required to initiate the motion of the motor operator drive sleeve. As shown in Fig. 5, the hammerblow current rise for this particular valve has varied considerably over the three-month time period shown; however, no consistent trend is apparent.

During this same time period, hammerblow transients were also observed infrequently on valve 8A. Unusual behavior was noted on isolated occasions in November and December, 1989 (see Fig. 6, where a more normal signature for this valve, obtained in January 1990, is shown for comparison). The November actuation shows a short-lived (~0.4 s duration) period of anomalously low running current (3.6-3.8 A) at the beginning of the open-to-close stroke. In December, two sharp transients were seen at the beginning of the open-to-close stroke, signifying the occurrence of two separate momentary load increases. The origin of these transients is unknown.

Figure 7 illustrates a small but discernible rise in motor current that occurs occasionally near the end of the open-to-close stroke of valve 7A (this feature has also been observed on valve 5B). The rise is not sufficiently abrupt to be an indication of valve seating, but is more likely attributable to an increase in valve internal friction resulting from a substantial increase in differential pressure across the valve obturator as it approaches the closed position.

2.2.1.3 Relay dropout. Occasionally, the valve 5A open-to-close signature has shown evidence of a motor trip and restart, which always occurs at 1.30 s from the beginning of the valve stroke. Fig. 8 illustrates this anomaly, which has been identified by plant personnel as faulty relay action. As a result of this finding, corrective actions have been taken by Eddystone.

2.2.1.4 Motor running current trends and variability. Table 2 documents trends observed in average running currents over a recent 4-month period of plant operation. It is recognized that measured changes in motor running current could merely be reflections of changes in line voltage; however, this does not seem likely, since only a few of the eight valves are seen to display any appreciable running current trend and, even then, the trends appear to depend on stroke direction (see Table 2). Moreover, the variability of running current is not the same for all valves. These observations tend to rule out power line variations as the underlying cause. It seems far more likely that the observed variations in running current are the result of changes in valve stem load caused by varying steam pressure, but this contention cannot be proved since extraction line pressures are not measured at the Eddystone plant.

The observation that, for most valves, the open-to-close stroke mean running current generally exceeds its close-to-open counterpart is explained by the increased stem load present in the closing direction due to internal valve pressure.

The relatively large variability of the average running current data makes trends difficult to discern, but some valves do show an undeniable trend. Valve 6B is an example; Fig. 9 shows its mean running current over a 3-month interval, plotted with an expanded ordinate scale for clarity. The linear fit for the entire 29-point data set indicates that this valve's running current in the close-to-open direction has been decreasing gradually with time. This same downward trend is, in fact, observed for the opposite stroke direction for valve 6B, but some of the other extraction valves display ascending trends for one stroke direction and descending trends for the other stroke direction.

Table 2. General Trends Observed in Mean Motor Current Measurements During the Period October 1989 through January 1990

Valve	Stroke	Mean (A)	Trend Observed
5A	Open-Close	5.30	Significant increase (0.25 A)
	Close-Open	5.24	No discernible trend
6A	Open-Close	3.35	No discernible trend
	Close-Open	3.32	No discernible trend
7A	Open-Close	1.68	No discernible trend
	Close-Open	1.63	No discernible trend
8A	Open-Close	5.14	Slight increase (0.08 A)
	Close-Open	4.91	Significant increase (0.22 A)
5B	Open-Close	2.53	No discernible trend
	Close-Open	2.55	No discernible trend
6B	Open-Close	2.84	No discernible trend
	Close-Open	2.91	Slight decrease (0.10 A)
7B	Open-Close	3.17	No discernible trend
	Close-Open	3.07	No discernible trend
8B	Open-Close	5.94	No discernible trend
	Close-Open	5.47	Slight decrease (0.11 A)

2.2.1.5 Valve stroke time trends and variability. Table 3 illustrates the manner in which valve stroke times have been observed to vary over the same 4-month time interval shown in the preceding section. An example of this variability is shown in Figure 10, which also illustrates the long-term trend observed for the same MOV actuations shown in Fig. 9. It was noted that the total variation in stroke time for 6B over this period was only 0.5 seconds; thus, stroke time measurements require a high precision technique (e.g., MCSA) if they are to provide meaningful diagnostic information. Changes in MOV stroke time can result from either altered motor speed (as a result of changed load) or altered valve stroke length. Assuming that the valve limit switches have not been changed since October 1989, the stroke lengths for a given stroke direction should be constant, leading to the conclusion that these trends in stroke time probably reflect changes in motor speed. To test this theory, motor speeds were determined from valve 7A demodulated motor current spectra acquired during several sequential open-to-close actuations. Motor slip values were then calculated as the difference between motor speed and 30 Hz (1800 rpm) and plotted, along with stroke times for these actuations (see Fig. 11). The obvious similarity between stroke times and motor slip verifies that the observed variations in valve stroke times result from variations in motor speed, rather than from changes in valve stem travel.

It is noted that all valves display a longer stroke time when closing than when opening. We believe that this is attributable to coasting at the conclusion of the closed-to-open stroke.

2.2.2 Frequency Domain Results

Frequency-domain analysis of current signals from the Unit 2 steam extraction valves has been attempted without much success except at such times when Unit 2 itself was not in operation. The difficulty encountered is that the 3-phase ac line supplying power to the MOVs is (for reasons unknown) heavily contaminated with noise whenever Unit 2 is in operation, and the non-MOV-related spectral peaks (predominantly 2 Hz and its higher harmonics) characterizing the unwanted power line noise completely mask most MOV-related spectral information occupying this same range of frequencies, as described in the following section. Frequency-domain analysis was applied successfully, however, in Unit 3 (see Section 2.1.4).

2.2.2.1 Unit 2 power line noise

Figs. 12 and 13 show motor current frequency spectra acquired both during Unit 2 operation and when the unit was shut down. In the latter case (Fig. 13), spectral peaks associated with well known motor operator functions are clearly identifiable, whereas in the former case (Fig. 12) they are obscured by the power line noise. Also shown are spectra representing only the noise on the power line supplying the MOVs; these data were acquired by analyzing the current passing through a purely resistive (dummy) load connected to the MOV power line, and using the same analysis method as employed for the MOVs. During Unit 2 operation, line-voltage noise of similar frequency structure was observed on both "A" and "B" train power busses, thereby masking most spectral features from all MOVs powered by these busses. It is important to realize that the presence of this electrical line noise may represent equipment difficulties within Unit 2. Accordingly, Eddystone personnel have taken steps to identify and correct this problem.

Table 3. General Trends Observed in Stroke Time Measurements During the Period October 1989 through January 1990

Valve	Stroke	Mean (s)	Trend Observed
5A	Open-Close	84.40	Slight decrease (0.12 s, 0.14%)
	Close-Open	82.96	No discernible trend
6A	Open-Close	46.57	Large but unvarying difference between stroke directions
	Close-Open	44.36	Large but unvarying difference between stroke directions
7A	Open-Close	22.64	Significant decrease (0.15 s, 0.66%)
	Close-Open	21.77	No discernible trend
8A	Open-Close	30.64	Significant decrease (0.26 s, 0.85%)
	Close-Open	29.76	Significant increase (0.18 s, 0.61%)
5B	Open-Close	59.26	Slight increase (0.23 s, 0.39%)
	Close-Open	58.79	Slight decrease (0.12 s, 0.20%)
6B	Open-Close	48.70	Extremely consistent performance
	Close-Open	47.92	Extremely consistent performance
7B	Open-Close	31.18	No discernible trend
	Close-Open	29.55	No discernible trend
8B	Open-Close	29.45	Significant increase (0.84 s, 2.9%)
	Close-Open	28.60	No discernible trend

2.2.2.2 MOV worm gear wear

As mentioned earlier, the MCSA method offers high sensitivity and selectivity for monitoring MOV operational characteristics. This is well exemplified by the application of SWIM (selective waveform inspection method). SWIM is a method of developing a signature that is representative of the time dependency of a specific periodic load. For example, this technique has been used to define the tooth meshing patterns of MOV worm gears [1]. In a similar manner, SWIM was used to investigate the worm gear tooth meshing characteristics of two Unit 3 MOVs, VP1 and VP6.

Figure 14 shows the demodulated motor current spectra for both of these valves over a 0 to 40 Hz range. Shown in the spectra are frequency peaks associated with motor slip, worm gear tooth meshing (both first and second harmonics), and motor shaft speed. The worm gear tooth meshing

(WGTM) frequency was different for the two MOVs due to differences in their motor operator gear trains.

Narrowband analog filters were employed to selectively eliminate all frequency content except the WGTM frequency in the recorded demodulated current signals for these two MOVs. The resulting signatures (Fig. 15), are plotted using expanded time scales in order to show three consecutive worm gear rotations for both valves. As shown in these plots, the amplitude of the WGTM frequency component is seen to vary with time with a recurrent pattern every 45 peaks for VP1 and every 50 peaks for VP6. These peak numbers correspond to the number of teeth on the worm gears of these motor operators; and thus, Fig. 15 reflects the worm gear tooth meshing characteristics of these two MOVs on a tooth-by-tooth basis.

In addition to the periodicity that occurs once per worm gear rotation, other variations in amplitude of the WGTM frequency are seen that correspond to irregular tooth meshing loads over various angular sectors of the worm gear. By numbering each peak sequentially (1 through 45 for VP1 and 1 through 50 for VP6), and averaging the amplitudes of each numbered peak over the three gear rotations, average peak amplitude polar plots were produced and are shown in Fig. 16. Previous SWIM applications by ORNL on a new MOV have shown that, when the worm gear is meshing with the worm in a consistent manner, the polar plot approaches a circle [1]. Thus, these plots illustrate that the worm gears in VP1 and VP6 are meshing with their respective worms in two distinctly different and irregular ways that may result in or be caused by worm gear wear.

2.3 Motor Current Signature Analysis of Other Rotating Machinery

Using portable test equipment rather than the ORNL on-line monitoring system, the use of motor current signatures for assessing the operating condition of a variety of motor-driven devices has been explored at Eddystone on a limited basis. The primary purpose of the measurements has been to establish baseline motor current signatures for selected machines in the event that operational difficulties develop later. Observations that can be drawn from the data collected to date are that (1) well-defined peaks (presumably caused by the occurrence of periodic mechanical load fluctuations within the machines) are evident in the motor current frequency spectra, (2) the spectra, while similar in overall characteristics for any given class of machine, have detailed features that are unique to individual machines of "identical" construction, and (3) time waveform analyses also yield trendable features that may be relevant to the operational condition of the equipment. These observations are consistent with the notion that useful performance and diagnostic data may be extractable in this manner from the motor current signals. Examples are treated briefly in the following sections.

2.3.1 Air Compressors

Motor current data were acquired on two Ingersoll-Rand type XLE air compressors during November, 1989. Both compressors were powered by 200-hp, 585-rpm electric motors rated at 253 A at 460 V.

One of the compressors had been recently refurbished. Figure 17 illustrates a motor current time trace during the startup of this compressor, showing that the compressor passes through two load conditions, (1) and (2), before reaching steady-state operation (3). Both the magnitudes of the current and the time duration during load conditions are condition indicators of the compressor itself and/or the compressed air system.

Figure 18 compares a portion of the steady-state time waveform for the two compressors on an expanded time scale and shows that the recently refurbished compressor draws more current than the non-refurbished one; thus, the refurbished compressor appears to be performing more work than the non-refurbished one. The running current magnitudes for both machines are seen to vary considerably ($\sim$130 A) during steady-state compressor operation, reflecting the large cyclic load characteristics of the compressors. Subtle but reproducible features seen in both time waveforms represent smaller running load characteristics common to both machines.

2.3.2 Induced-Draft Fans

Figure 19 illustrates the frequency spectra of demodulated motor current signals acquired essentially simultaneously from two nominally identical 1190-rpm, direct-drive, induced-draft fans. The motor loads imposed by the two fans were the same, within the accuracy of the current indicating meter. The spectral ordinate values have been plotted on a 4-decade logarithmic scale to best display salient features, such as the broad resonance located at about 24.5 Hz, the physical cause of which is presently unknown but clearly reflects an operational characteristic common to both machines. It is noted that this broad resonance was absent in demodulated current spectra of other machines, thus ruling out power line noise as an explanation. The increased spectral amplitudes at the lower frequencies are a common characteristic of fans and pumps, and are indicative of hydrodynamic phenomena. Many of the narrow, equi-spaced peaks so prominent in the frequency range 8 to 20 Hz may represent power line noise rather than features introduced by the fans.

2.3.3 Faulted Motor Demonstration Rig

Electric current signals were acquired from a test rig available at the EPRI M&D Center consisting of two 1-hp, 1725-rpm motors mechanically connected by drive belts of equal length to a single ac generator which could be electrically connected, as desired, to a 975-W load [5]. The two motors were identical in construction but one had been purposely faulted by cutting four consecutive rotor bars of its armature, thereby simulating one type of naturally occurring motor defect.

Useful diagnostic information related to motor condition was obtained by examining periodic current features in the frequency domain, where prominent peaks are seen corresponding to such electrical and mechanical phenomena as motor slip, belt rotation, and motor shaft rotation. As shown in Figs. 20 and 21, loading each motor with the electric generator resulted in spectral changes, including slower motor shaft speed, increased slip (hence, greater slip frequency), and increased magnitude of the belt passing frequency amplitude (indicating increased belt load). The amplitude of the slip frequency increased in both the good and the bad motor when operating under load; however, the good motor showed only a minor increase, whereas the bad motor's slip frequency peak under load was at a level over 5 times that seen under no load.

It is recognized that the use of motor current for detecting broken rotor bars and other types of motor degradation has been documented by others [6] and consists primarily of examining the amplitude of motor slip sidebands that are observed around the 60-Hz power line frequency in the undemodulated motor current noise spectrum. The presence of broken rotor bars is known to increase the induced currents in the stator windings, resulting in increased slip sideband amplitudes [7]. However, this same diagnostic information is also present in the "demodulated" motor current noise spectrum found useful for identifying problems in MOVs. The relationships between the two analysis techniques are shown in Fig. 22 for the bad motor operating under full load. Many of the same electrical and mechanical phenomena may be seen in both spectra; however, the differences in extractable information content between the two types of displays are substantial, based on the additional sensitivity that is realized when the raw signal is demodulated prior to recording on analog magnetic tape or displaying on a frequency analyzer. For example, Fig. 22 shows that the slip sidebands appear ~45 dB below the 60-Hz line frequency peak; however motor diagnostic information can still be seen in the demodulated spectrum at over 35 dB below the slip peak. The use of demodulation permits meaningful information to be obtained, even with the dynamic range limitations imposed by an analog tape recorder, at 80 (45 + 35) dB below the 60-Hz power line carrier frequency peak. Indeed, others [8] have indicated that a dynamic range of 110 dB (carrier amplitude to noise floor) is achievable using demodulation techniques.

The ability to see not only the slip frequency peak but also less prominent spectral characteristics becomes more difficult as the motor is less loaded (and/or when the motor is in better condition). For example, the slip peak amplitude for the good motor under no load was determined to be only one-twelfth as large (0.007 A) as the slip peak amplitude of the bad motor operating under load (0.088 A). Thus, when using motor current noise spectra as a diagnostic of the motor and/or the driven device, it is useful to demodulate the raw current signal prior to recording or analyzing, since the dynamic range of the analysis is thereby increased.

3. CONCLUSIONS AND PLANS FOR FURTHER WORK

Analyses of motor-operated steam extraction valve performance to date have identified several features and trends whose operational significance should become more apparent with the accumulation of additional long-term data, aided by maintenance information and discussions with Eddystone Generating Station personnel. The potentially most significant finding to date is that none of the eight MOVs shows any sign of complete closure, owing to the choice of limit switch (rather than torque switch) drive motor shut off. A second notable observation is that the reliable performance of at least one valve operator seems to be compromised by an incorrectly adjusted or maintained relay. A third observation is that at least two valve operators often show considerable hammerblow loads, even though the valves themselves are not hard seated; this may be a sign of improper lubrication or stem/stem nut thread wear and warrants further investigation.

The use of SWIM (selective waveform inspection method) identified irregular worm gear tooth meshing characteristics of two MOVs. Also, identification of significant noise on the Unit 2 power line has prompted Eddystone to begin an investigation into the source of this phenomenon, since it may represent difficulties associated with a particular piece of equipment within Unit 2.

The acquisition of motor-current signatures from other plant equipment (boiler and condensate feed pumps, induced-draft fans, air compressors, and mills) has provided baseline signatures containing a large number of spectral peaks which will require additional discussions with Eddystone and EPRI M&D Center personnel, as well as examination of equipment design details, to determine the diagnostic significance of such data.

The uses of demodulated motor current spectra to detect broken rotor bars in a degraded motor was also demonstrated. The application of MCSA thus was shown to be valuable not only to diagnosing problems in driven devices (valves, compressors, fans, etc.) but in diagnosing problems in the motor itself.

In addition to acquiring more data on the steam extraction valves and selected plant equipment in the future, current plans include making improvements to the on-line monitoring system (such as real-time screen displays, automated parameter extraction and trending, and on-line MOV diagnostics) which will increase its usefulness to the Eddystone operators and the M&D Center staff.

4. ACKNOWLEDGEMENTS

Funding for this work was provided by the Director's Discretionary Fund of the Oak Ridge National Laboratory, which underwrites the program carried out by the Advanced Diagnostic Engineering R&D Center. The authors gratefully acknowledge the cooperation and technical assistance provided by both Eddystone Generating Station and EPRI M&D Center personnel in carrying out this continuing investigation. The assistance of Jeanie Shover and Kathy Sharp in preparing this manuscript is also greatly appreciated.

5. REFERENCES

[1] H. D. Haynes, *Aging and Service Wear of Electric Motor-Operated Valves Used in Engineered Safety-Feature Systems of Nuclear Power Plants - Volume II, Aging Assessments and Monitoring Method Evaluations*, NUREG/CR-4234 (ORNL-6170/V2).

[2] R. C. Kryter and H. D. Haynes, "Condition Monitoring of Machinery Using Motor Current Signature Analysis," Sound and Vibration, pp. 14-21 (September 1989).

[3] H. D. Haynes, R. C. Kryter, C. Lacombe, and C. P. Stafford, *Informal Report on Activities in Progress at the EPRI M&D Center*, ADEC-P1, November 10, 1989.

[4] H. D. Haynes and B. K. Stewart, *Second Informal Report on Activities in Progress at the EPRI M&D Center*, ADEC-P2, March 20, 1990.

[5] H. D. Haynes, *Detection of Broken Rotor Bars in a Defective Motor Using Motor Current Signature Analysis*, ADEC-P3, May 16, 1990.

[6] G. B. Kliman and J. Stein, "Inductive Motor Fault Detection Via Passive Current Monitoring-A Brief Survey," *Proceedings of the 44th Meeting of the Mechanical Failures Prevention Group, Virginia Beach, Virginia, April 3-5, 1990.*

[7] J. Reason, "Pinpoint Induction-Motor Faults by Analyzing Load Current," *Power Magazine*, October 1987.

[8] S. F. Smith, K. N. Castleberry, and C. H. Nowlin, "Machine Monitoring Via Motor-Current Demodulation Techniques," *Proceedings of the 44th Meeting of the Mechanical Failures Prevention Group, Virginia Beach, Virginia, April 3-5, 1990.*

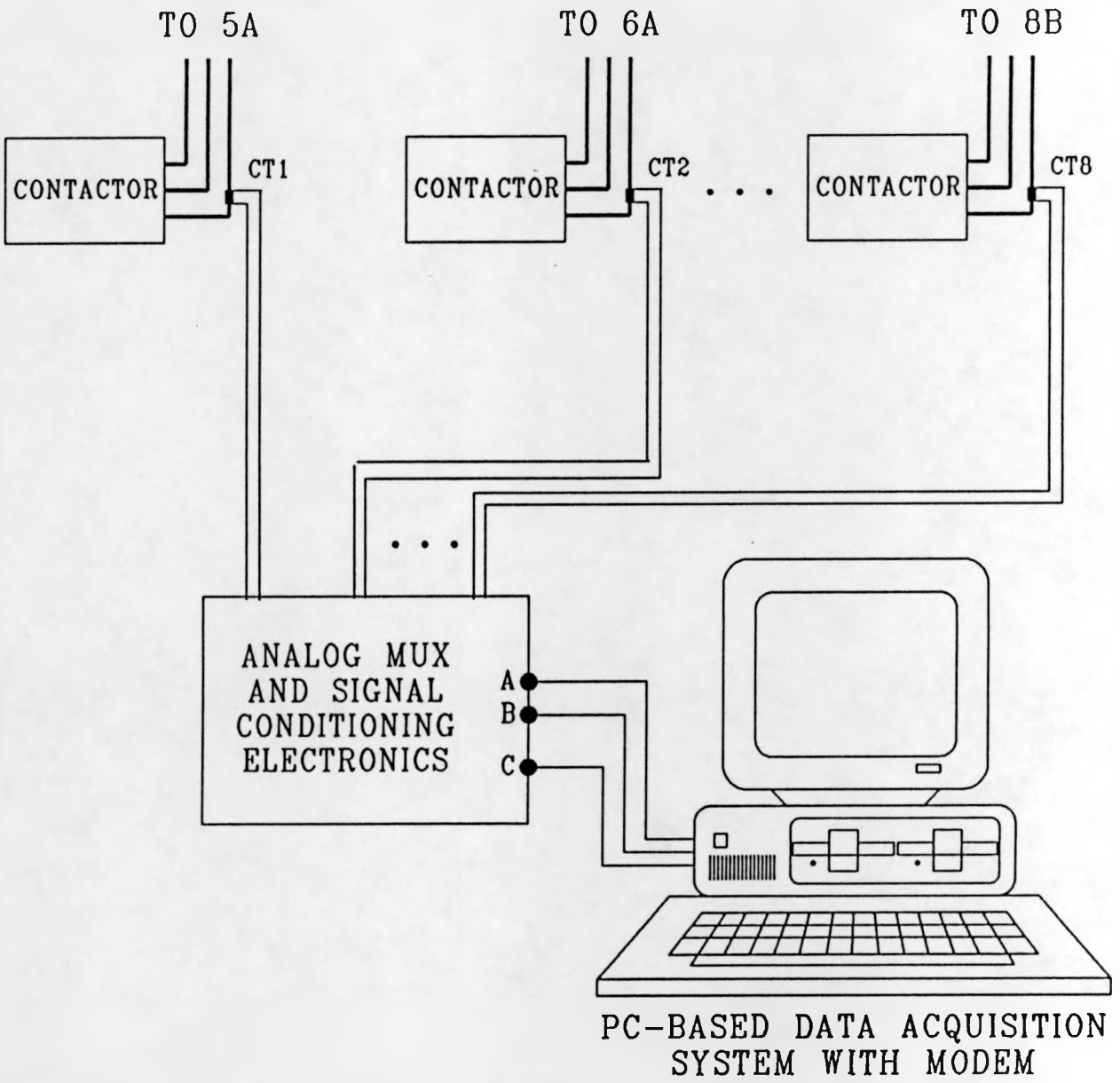

Fig. 1 Schematic diagram of ORNL/ADEC Steam Extraction Valve Performance Monitoring System. "A" and "B" are analog signals optimized for time- and frequency-domain analyses, respectively; "C" is a digital signal supplying valve identification.

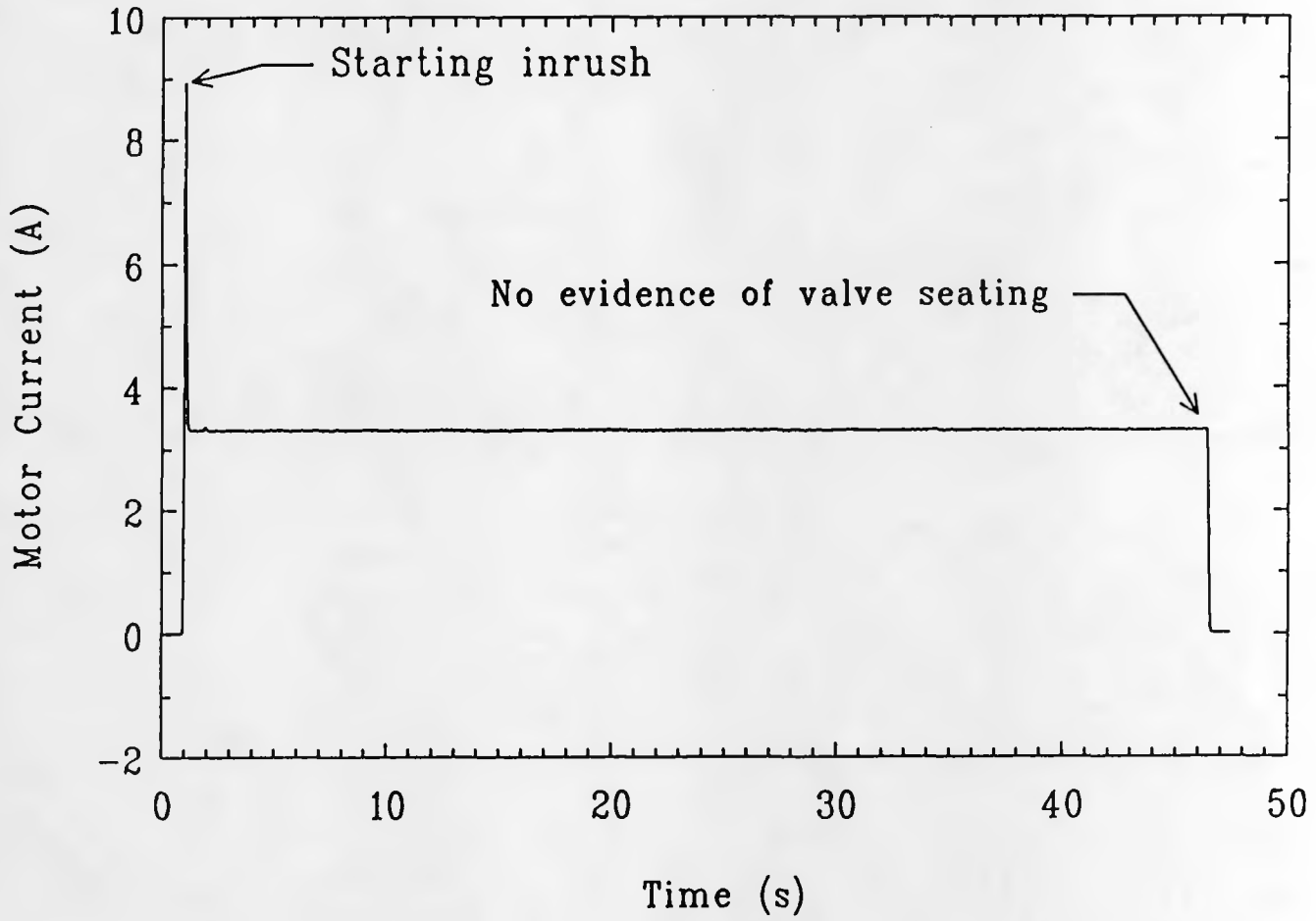

Fig. 2 Typical time-domain motor current trace for an open-to-close stroke of Unit 2 extraction valve 6A.

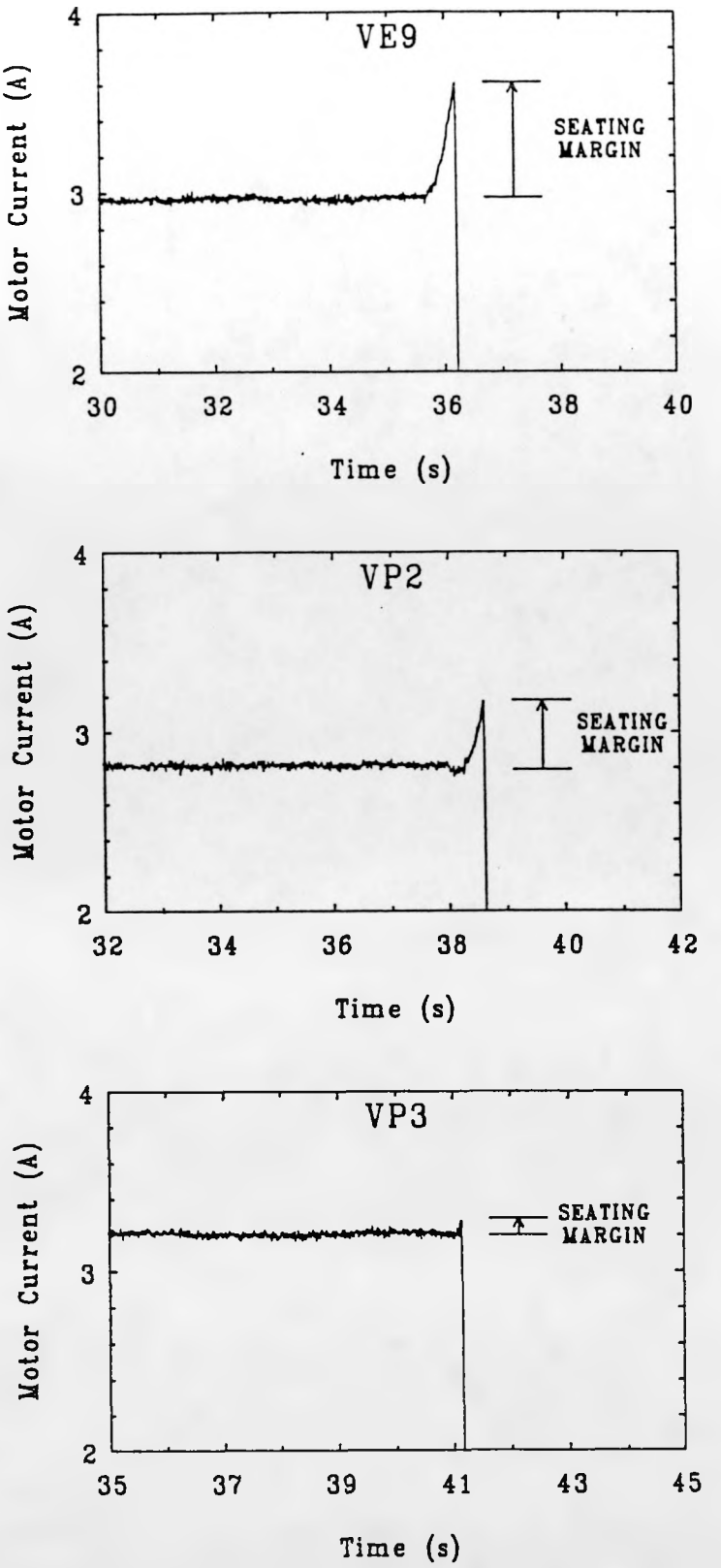

Fig. 3 The last few seconds of the open-to-close strokes of three Unit 3 valves, plotted with expanded current scales. The rise in motor current at the end of each stroke indicates that all three valves seated; however, valve VP3 is seen to seat with a lesser margin than the other two valves.

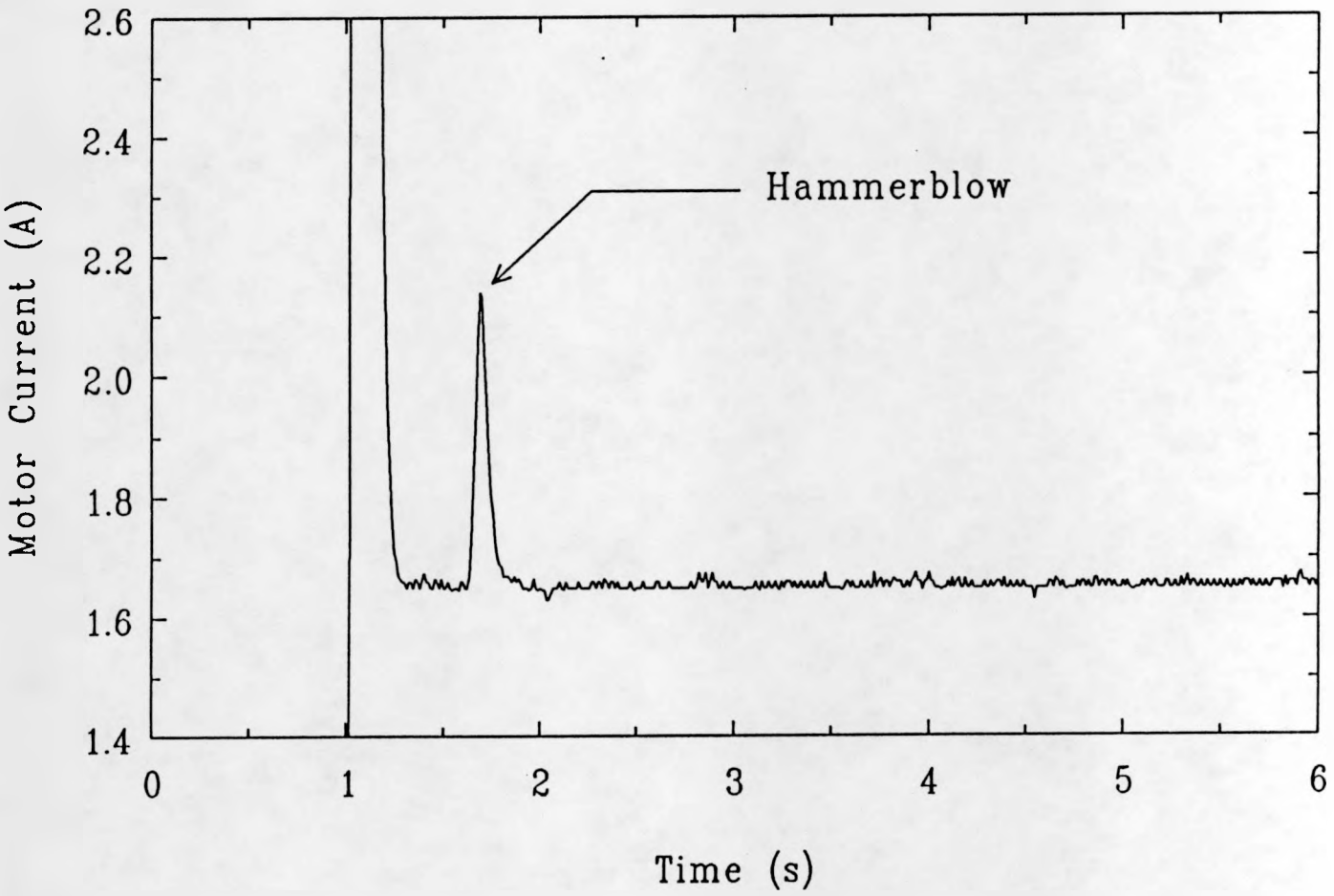

Fig. 4 Initial portion of an open-to-close stroke of Unit 2 valve 7A in January 1990, showing the occurrence of a prominent operator hammerblow ~ 0.6s after motor startup.

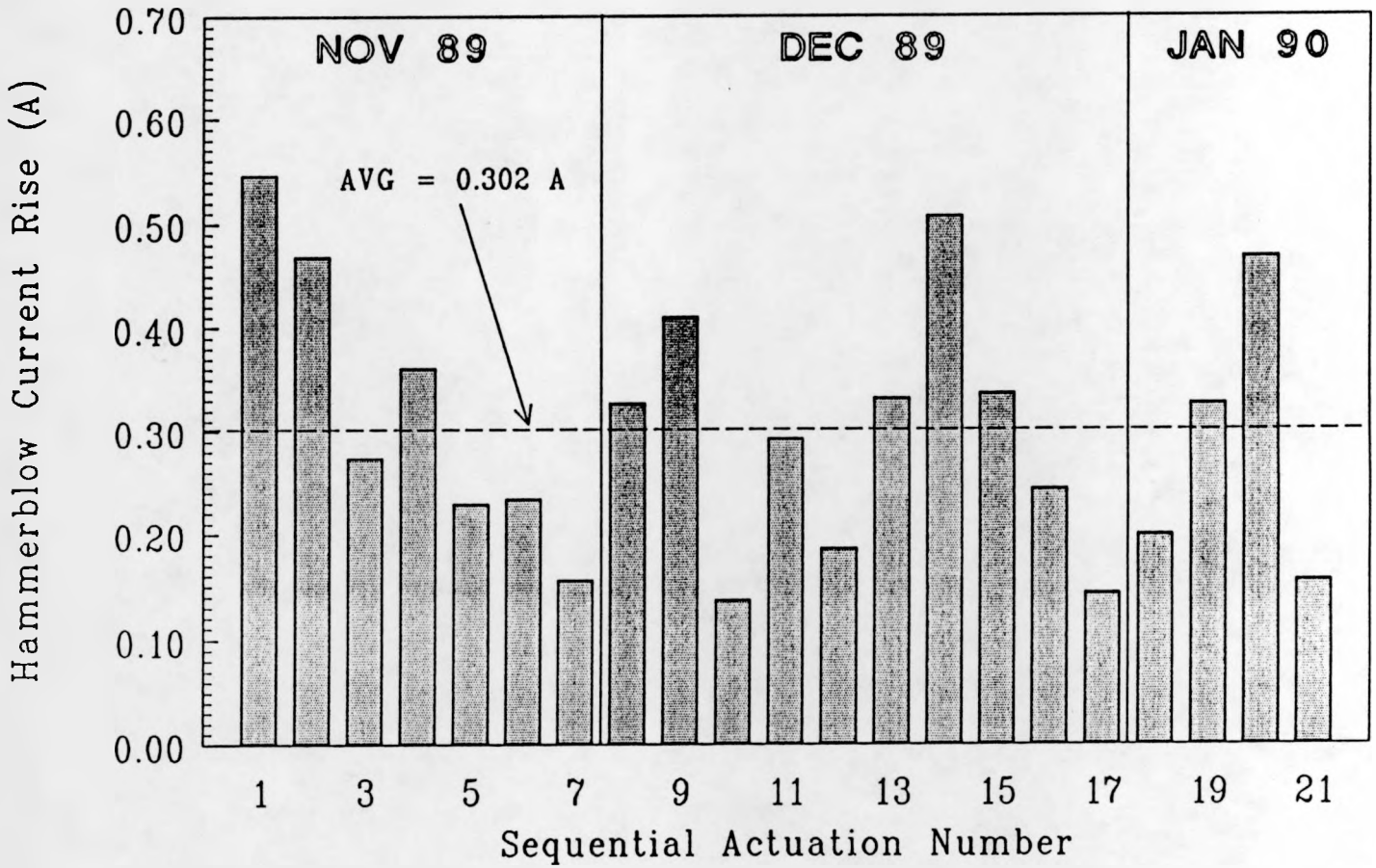

Fig. 5 Variations in amplitude of hammerblow current observed for valve 7A over a 3-month period.

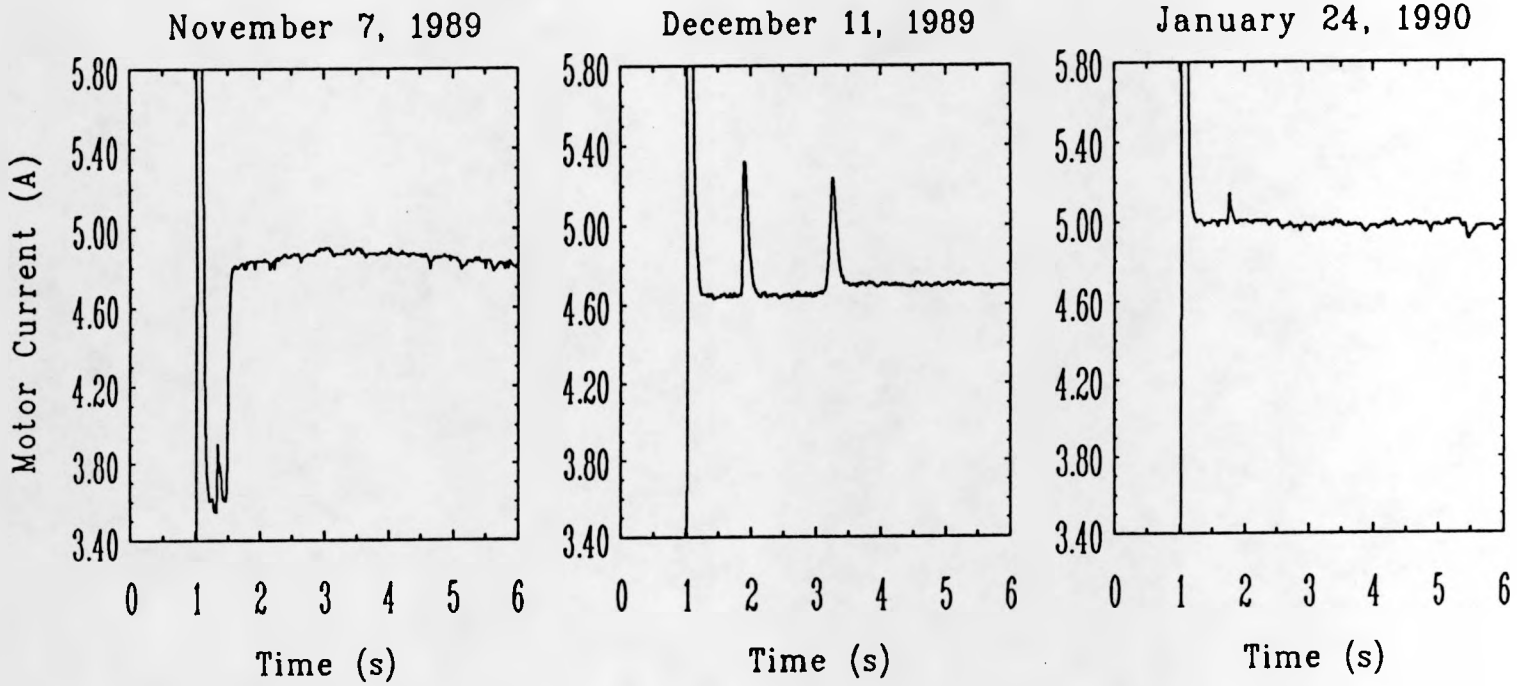

Fig. 6 Three different time-domain motor current signatures observed for Unit 2 valve 8A. The initial portions of the open-to-close stroke directions are shown, plotted with an expanded current scale.

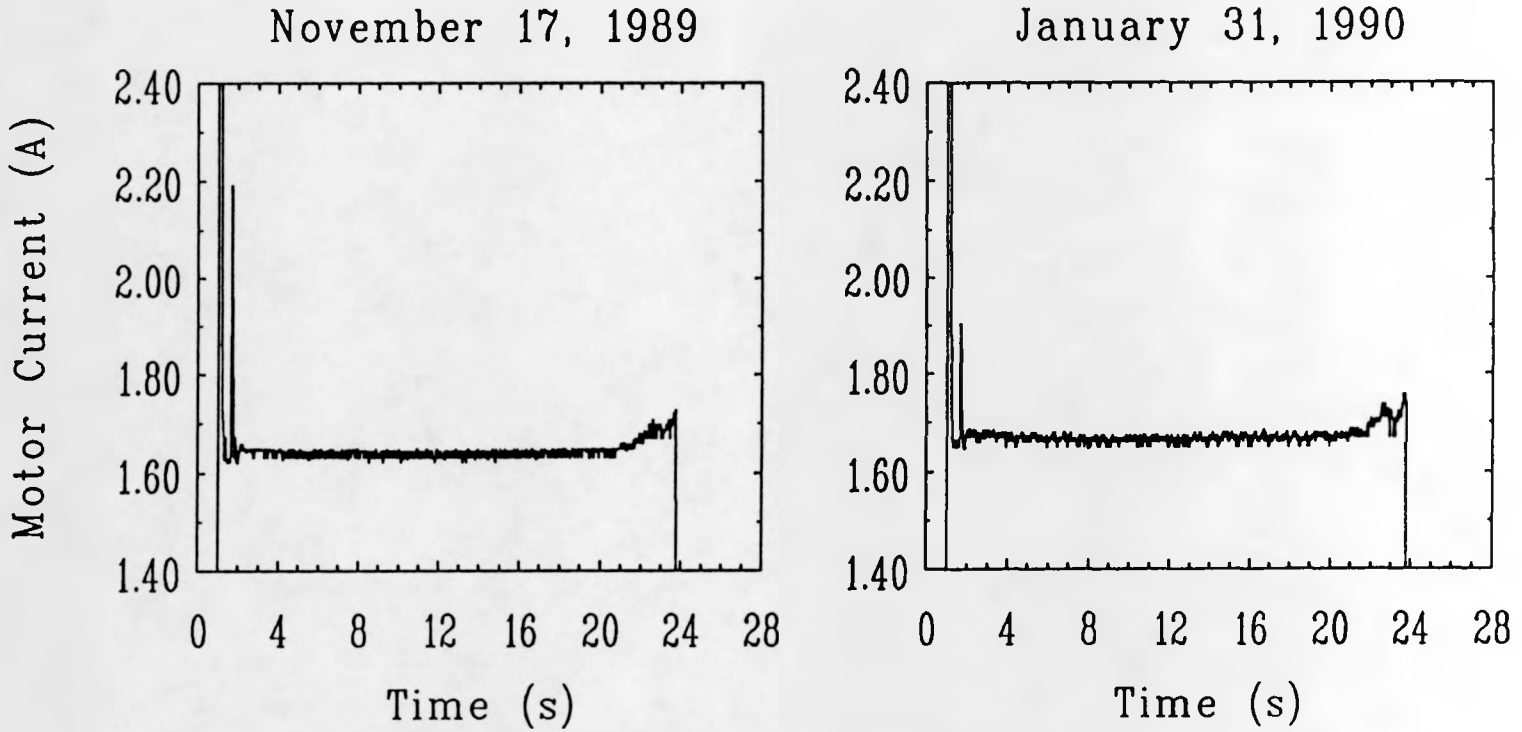

Fig. 7 Slow, small rise in motor current sometimes observed near the end of the open-to-close stroke of Unit 2 valve 7A. The rise is not sufficiently rapid or large enough to be an indication of valve seating; compare to Fig. 3.

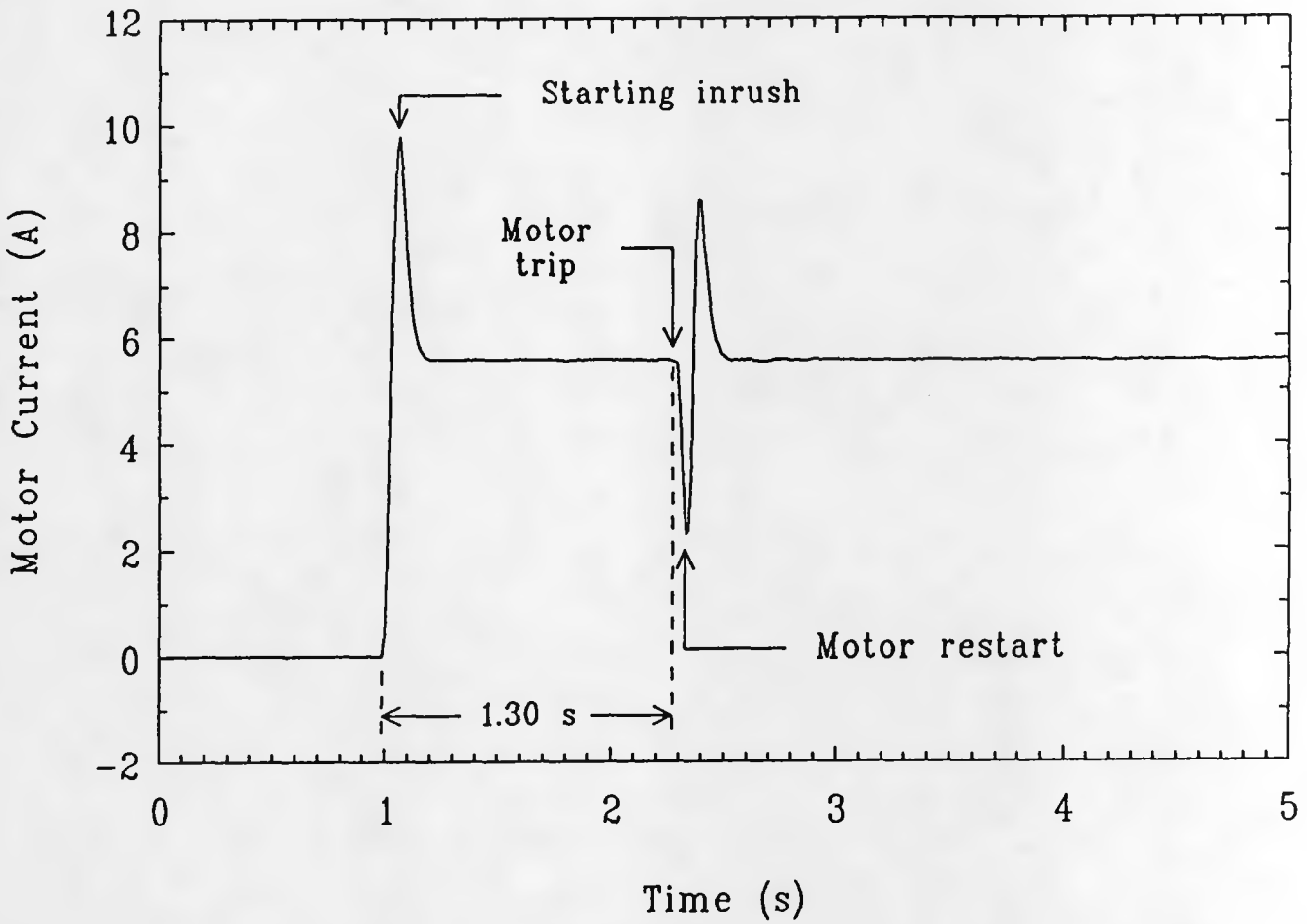

Fig. 8 Motor trip and subsequent restart of Unit 2 valve 5A in the open-to-close stroke direction, observed repeatedly in October 1989.

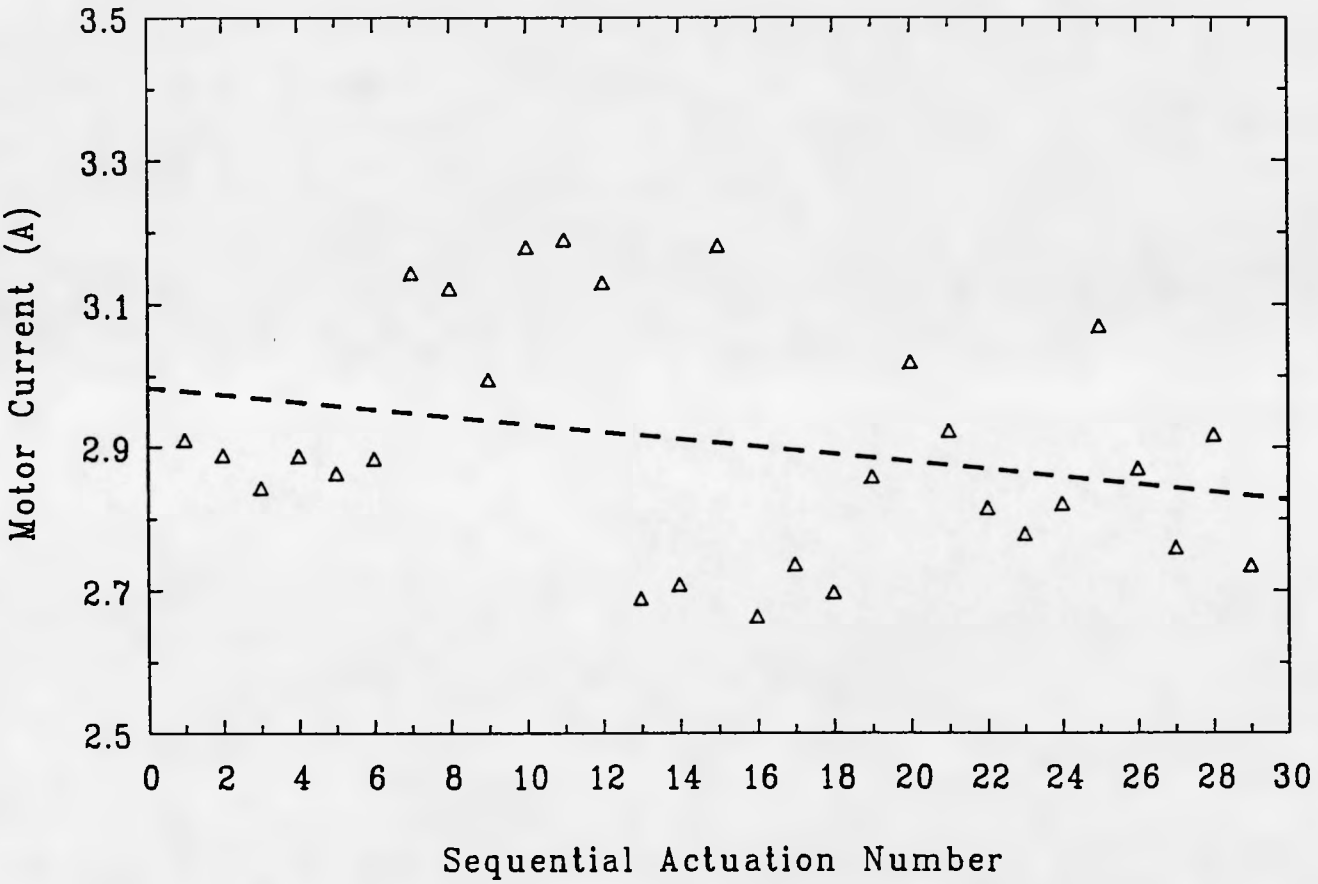

Fig. 9 Average running current for time-ordered actuations of Unit 2 valve 6B in the close-to-open stroke direction over a three-month period, plotted with an expanded current scale. The dashed, descending line shows the best linear fit to the entire data set.

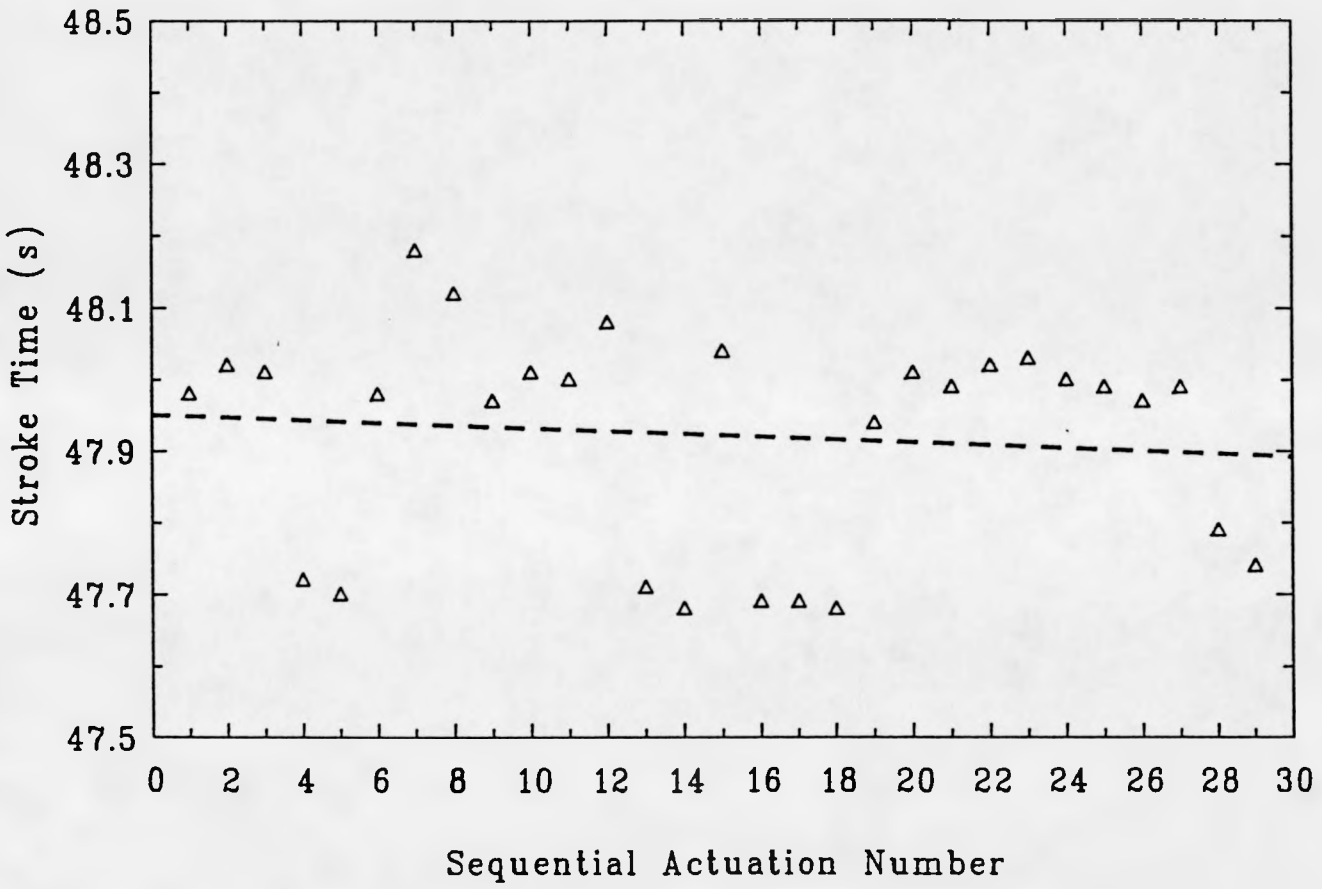

Fig. 10 Stroke times for the same actuations of Unit 2 valve 6B shown in Fig. 9 plotted with an expanded time scale. The dashed, descending line shows the best linear fit to the entire data set.

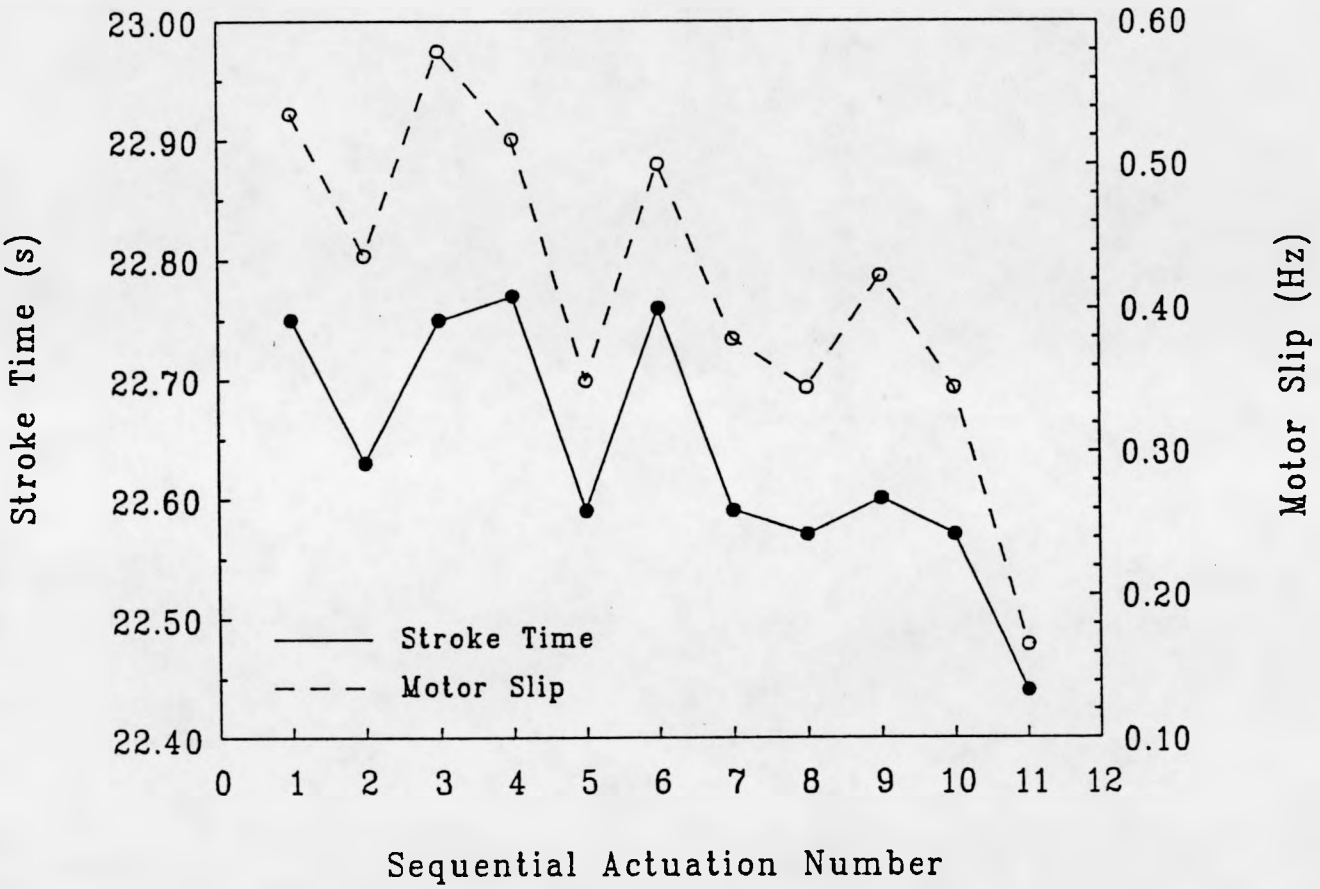

Fig. 11 Stroke time and motor slip values obtained from Unit 2 valve 7A open-to-close stroke motor current data, plotted with expanded scales. The similarity between stoke time and slip plots indicates that variations in valve stroke time result from variations in motor speed, not from variations in valve stem travel.

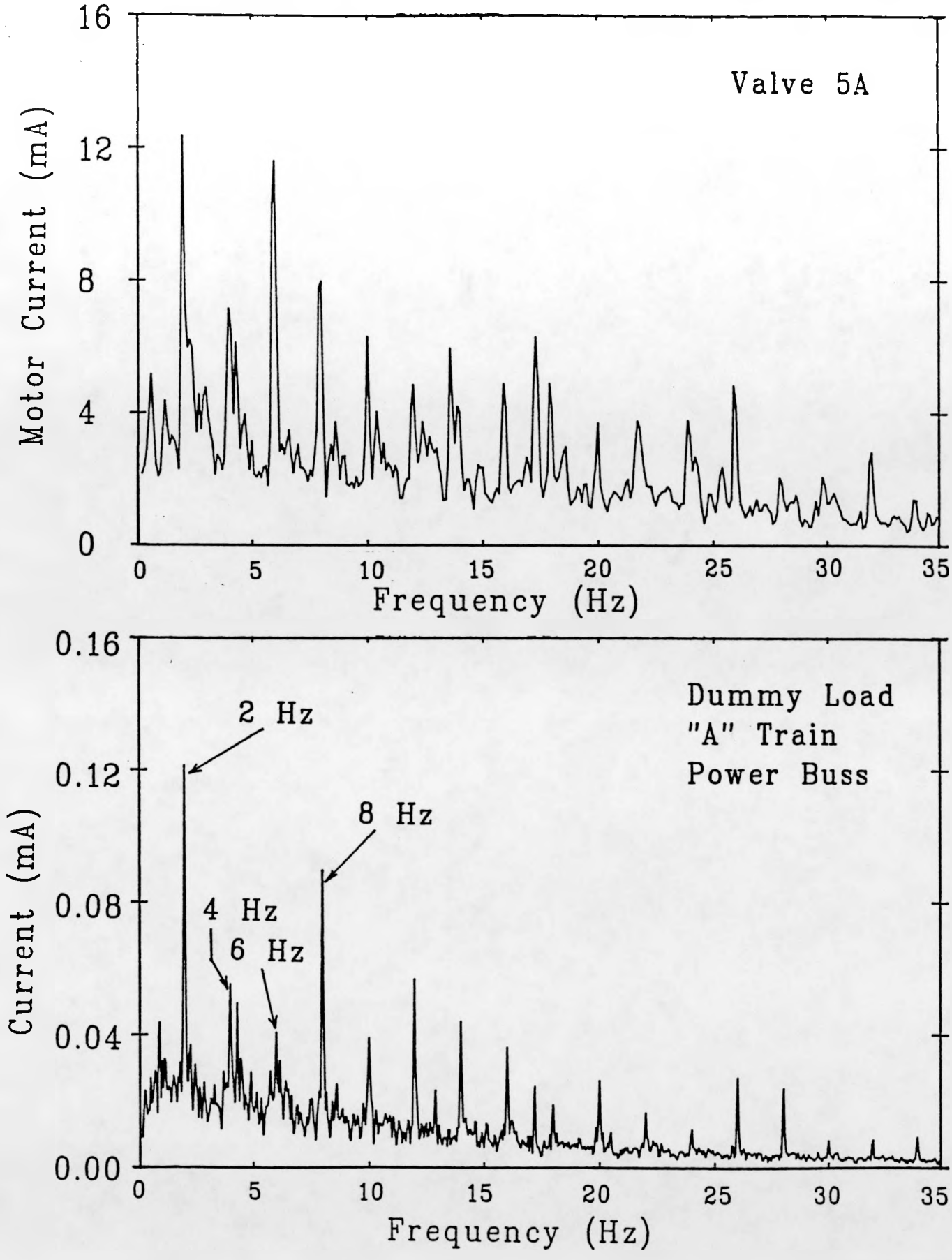

Fig. 12 Frequency-domain demodulated motor current trace (spectrum) for the close-to-open stroke direction of Unit 2 valve 5A. Shown for comparison is the spectrum of the noise on the power line supplying this valve. Unit 2 was operating at full power when these data were acquired.

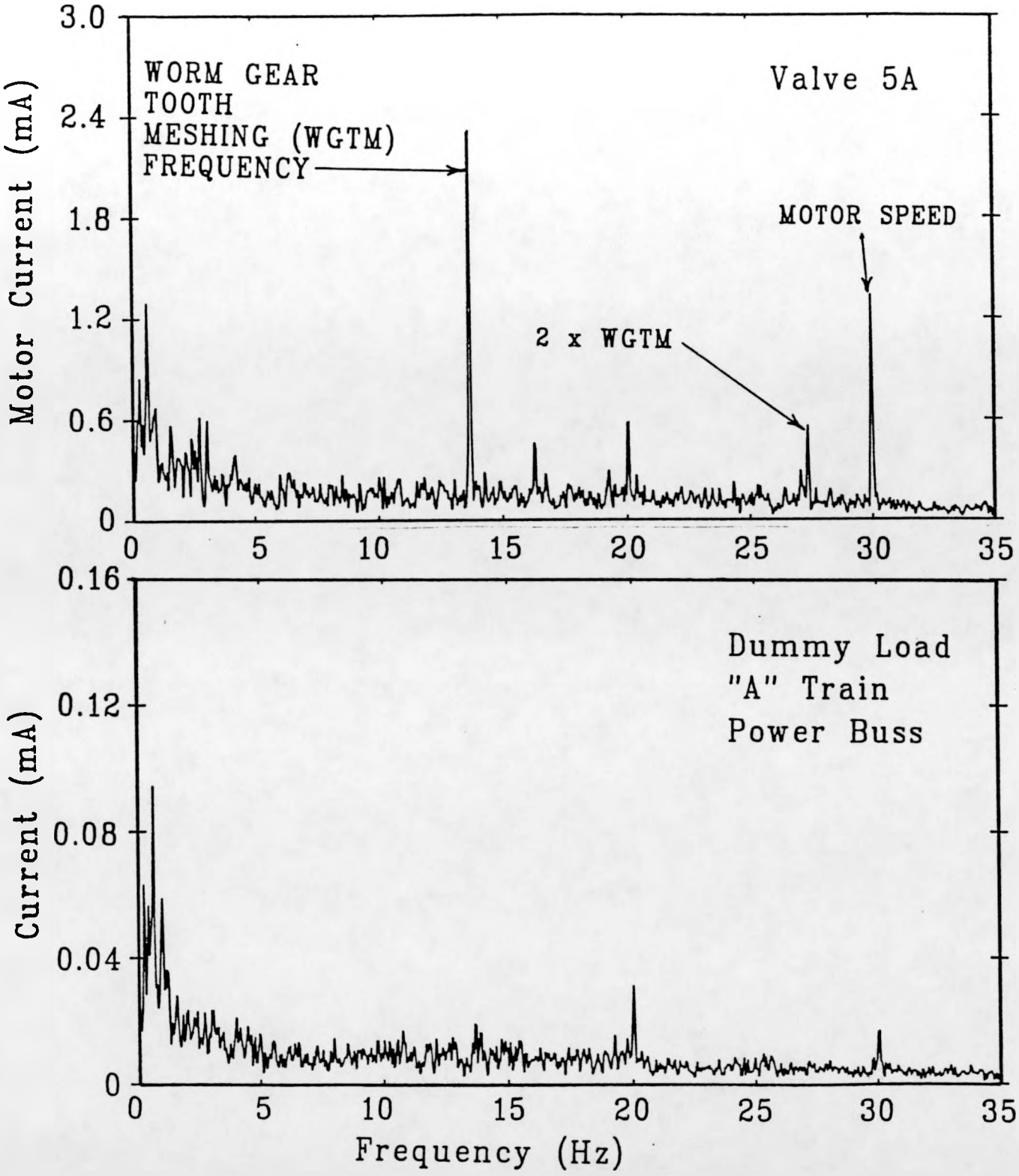

Fig. 13 Demodulated motor current spectrum for the close-to-open stroke direction of Unit 2 valve 5A, along with a comparison spectrum of the noise in the power line supplying this valve. Unit 2 was shut down for maintenance when these data were acquired.

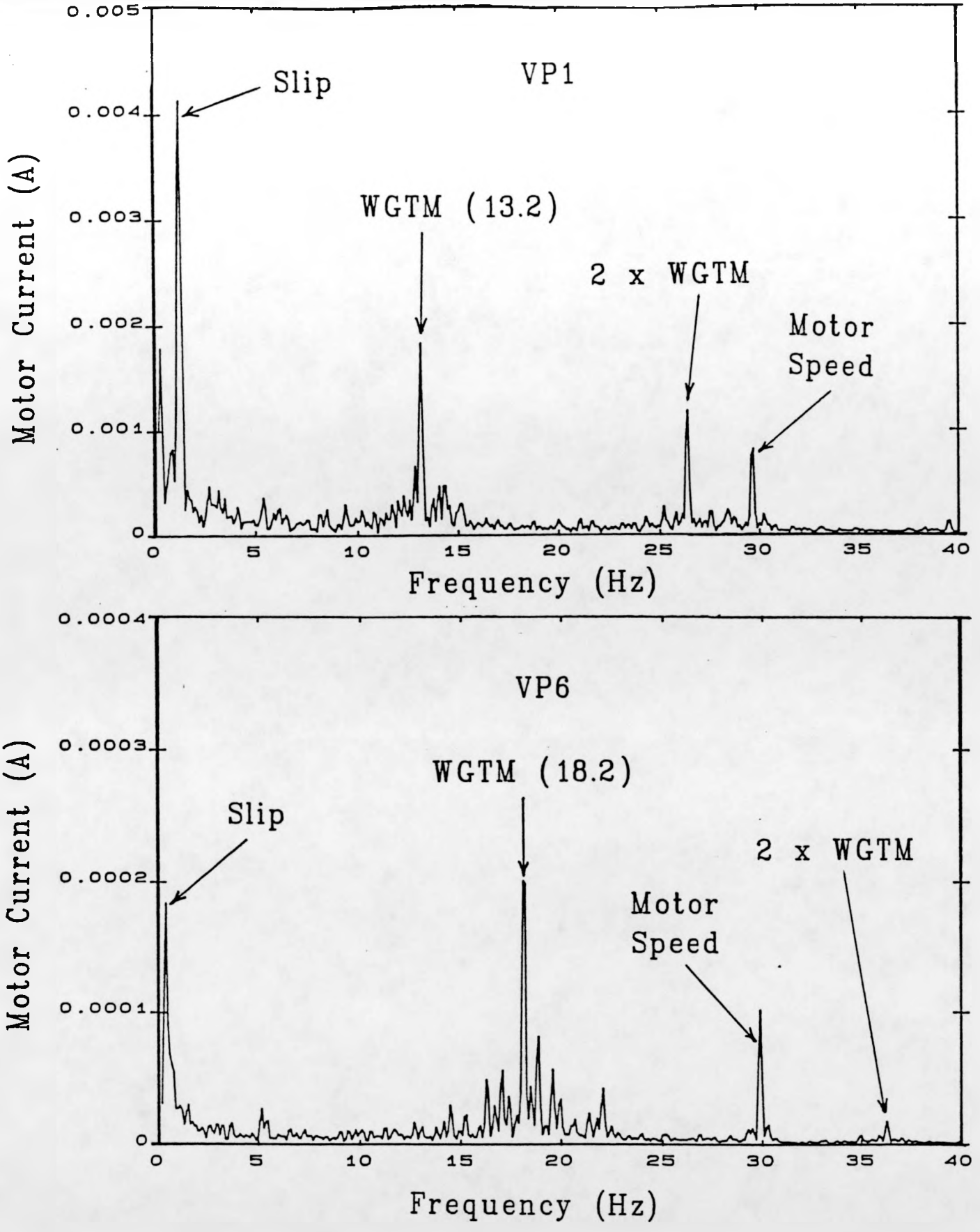

Fig. 14 Demodulated motor current spectra from two Unit 3 valves; VP1 and VP6. Both spectra contain several identifiable peaks indicative of the operational condition of each MOV. The worm gear tooth meshing (WGTM) frequency is different for the two MOVs due to differences in motor operator gear trains.

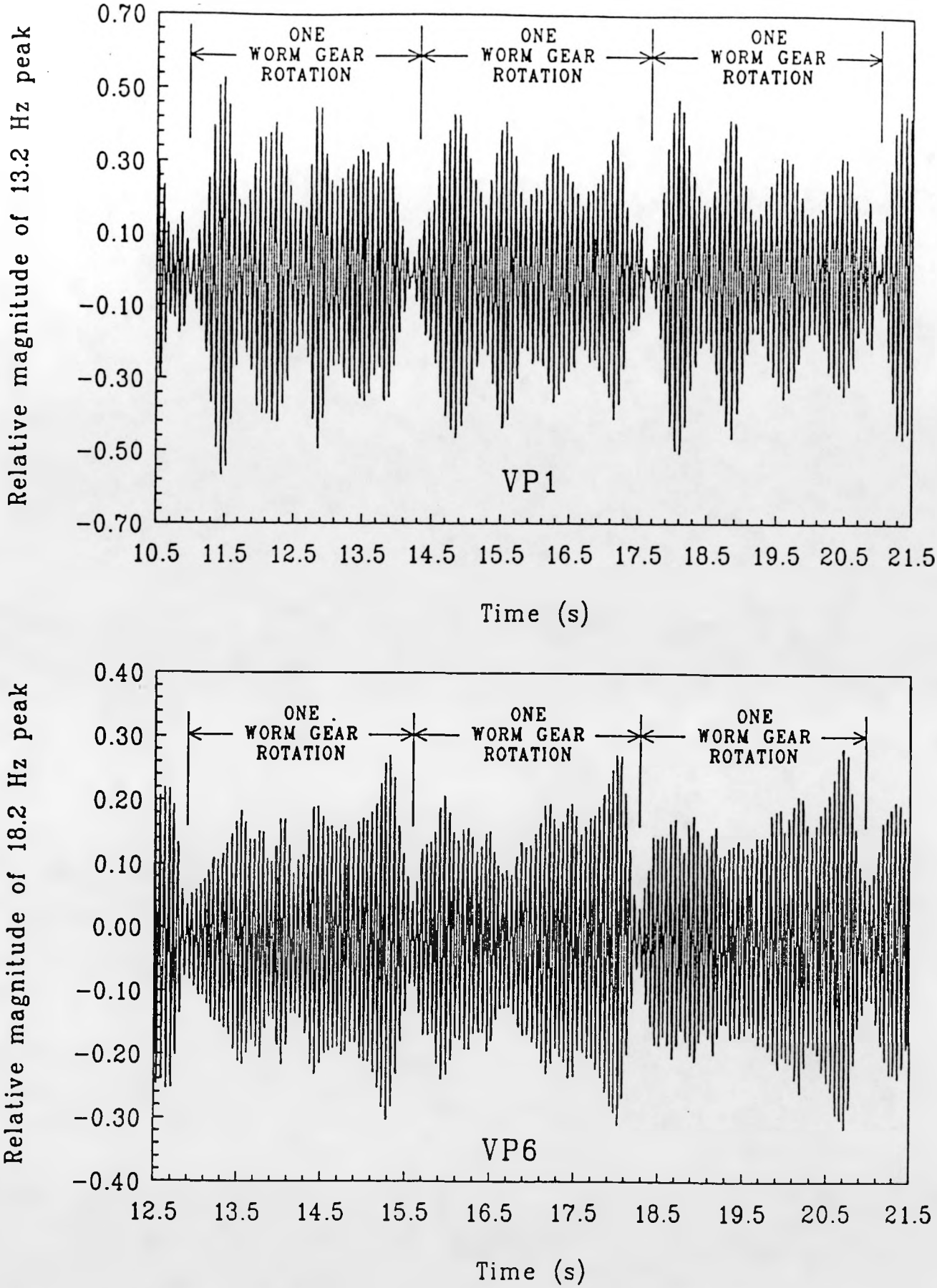

Fig. 15 Application of SWIM (Selective Waveform Inspection Method) to the demodulated current data represented by the two spectra in Fig. 14. The amplitude modulations of the worm gear tooth meshing frequencies indicate that the worm gears of Unit 3 valves VP1 and VP6 are meshing irregularly.

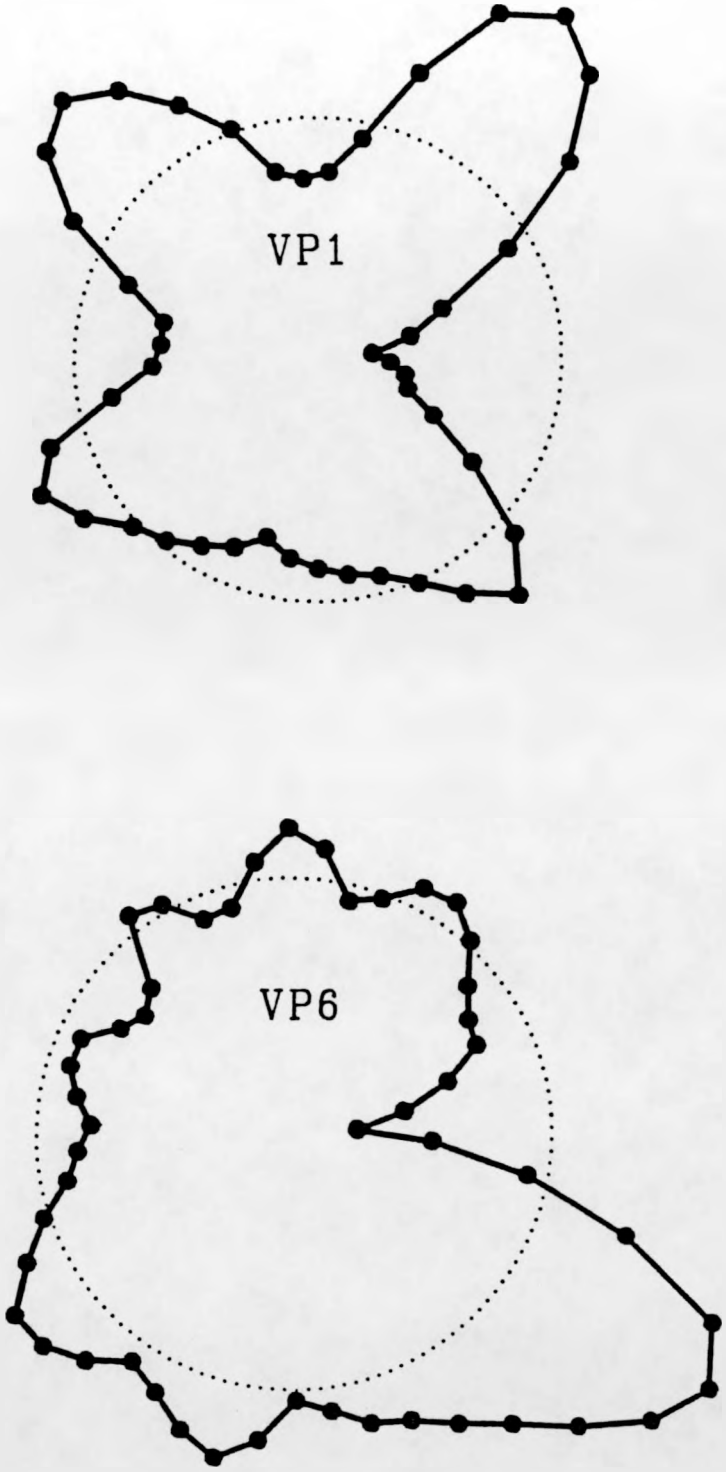

Fig. 16 Polar plot representations of the worm gear tooth meshing patterns shown in Fig. 15, illustrating gear meshing irregularities of valves VP1 and VP6 are associated with angular sectors of their respective worm gears.

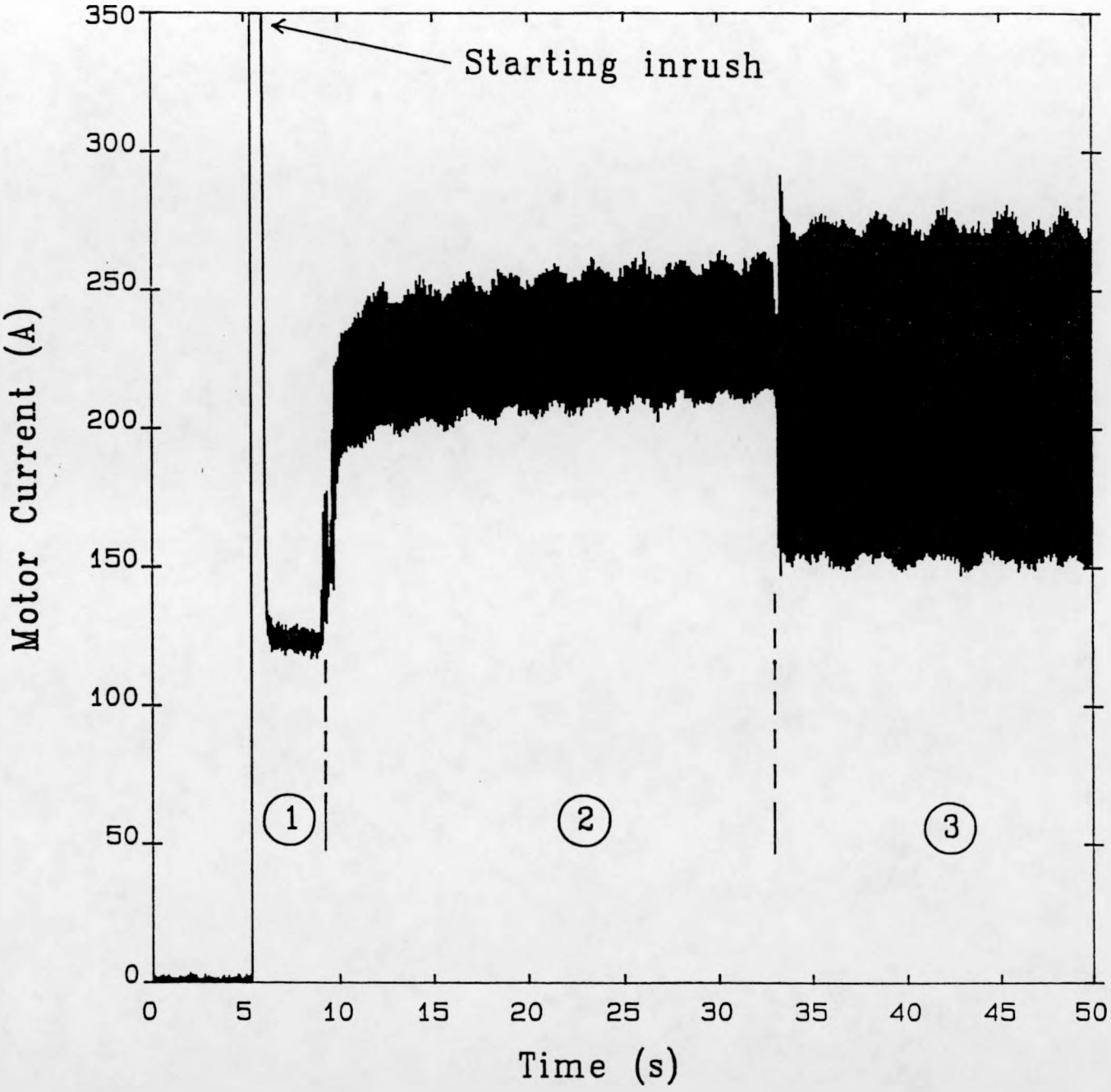

Fig. 17 Motor current time waveform for the reburbished air compressor acquired during its startup. The compressor is seen to pass through two periods (1 and 2) of reduced load prior to achieving steady-state operation (3) characterized by current oscilations of increased amplitude.

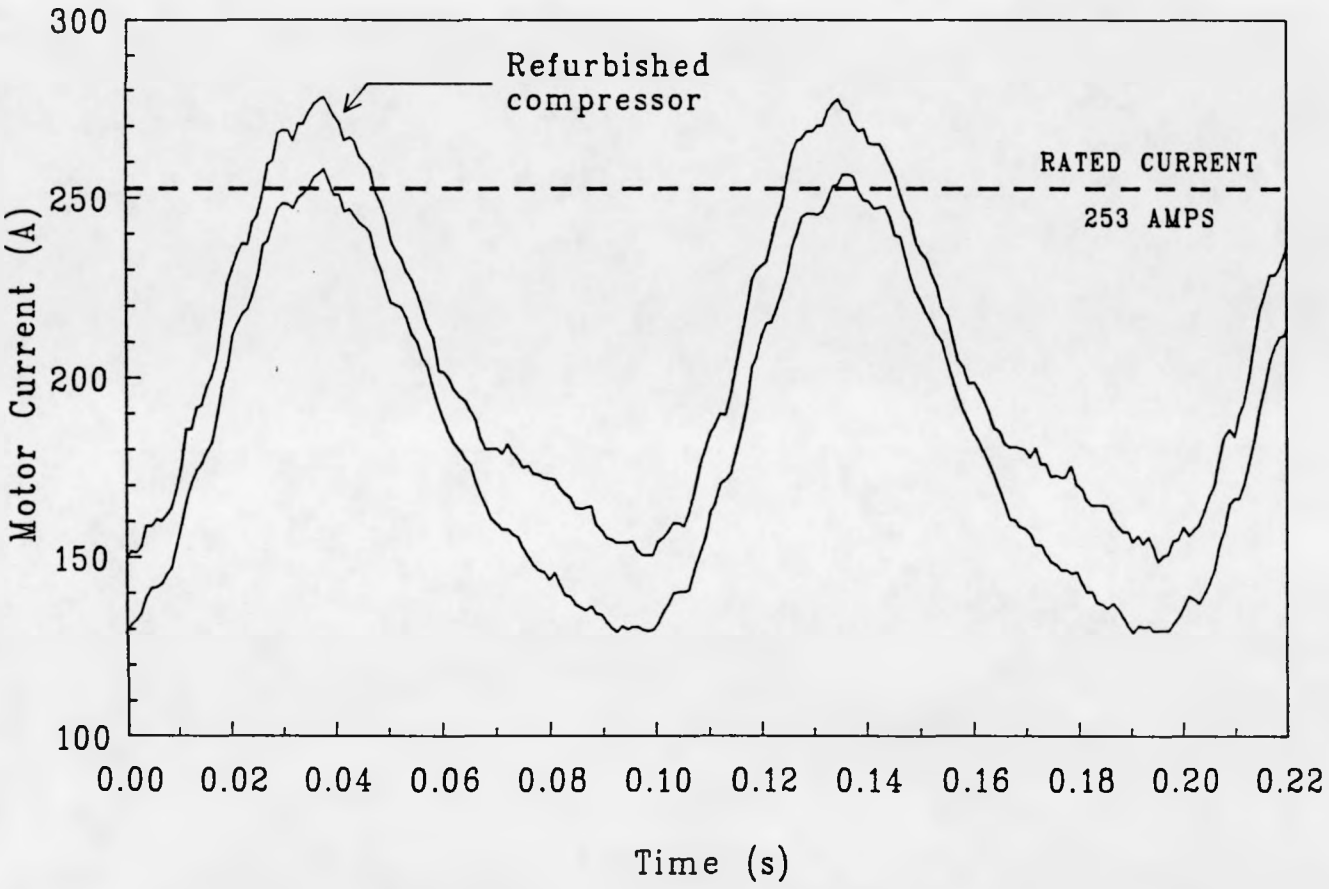

Fig. 18 Motor current time waveforms for two air compressors. The refurbished compressor draws greater peak and average currents during operation than does the other compressor, indicating that it performs more compressive work.

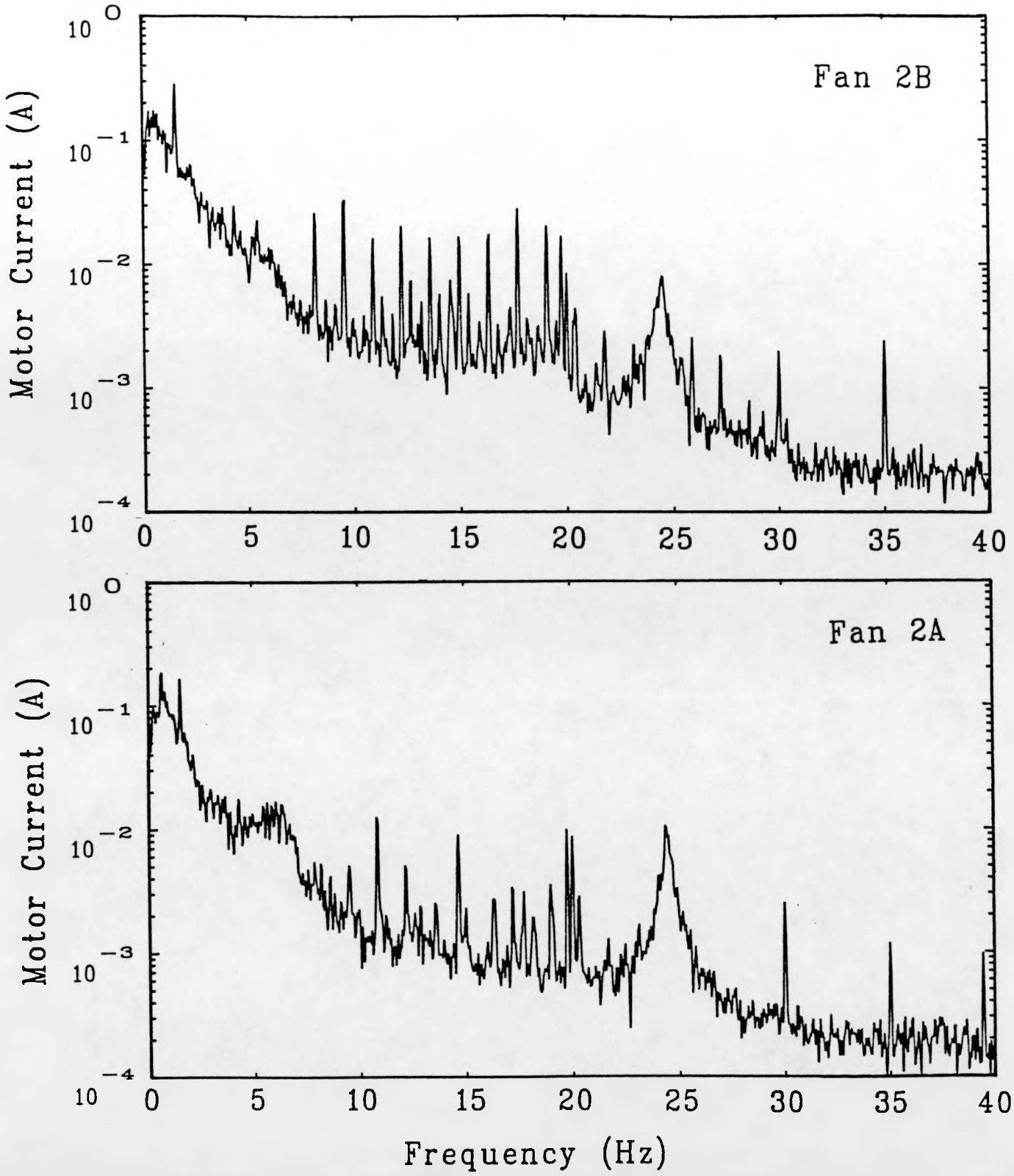

Fig. 19 Demodulated motor current spectra for Unit 2 induced-draft fans 2A and 2B, plotted with a four-decade logarithmic vertical scale to better illustrate low-amplitude peaks. The two spectra were acquired within five minutes of each other.

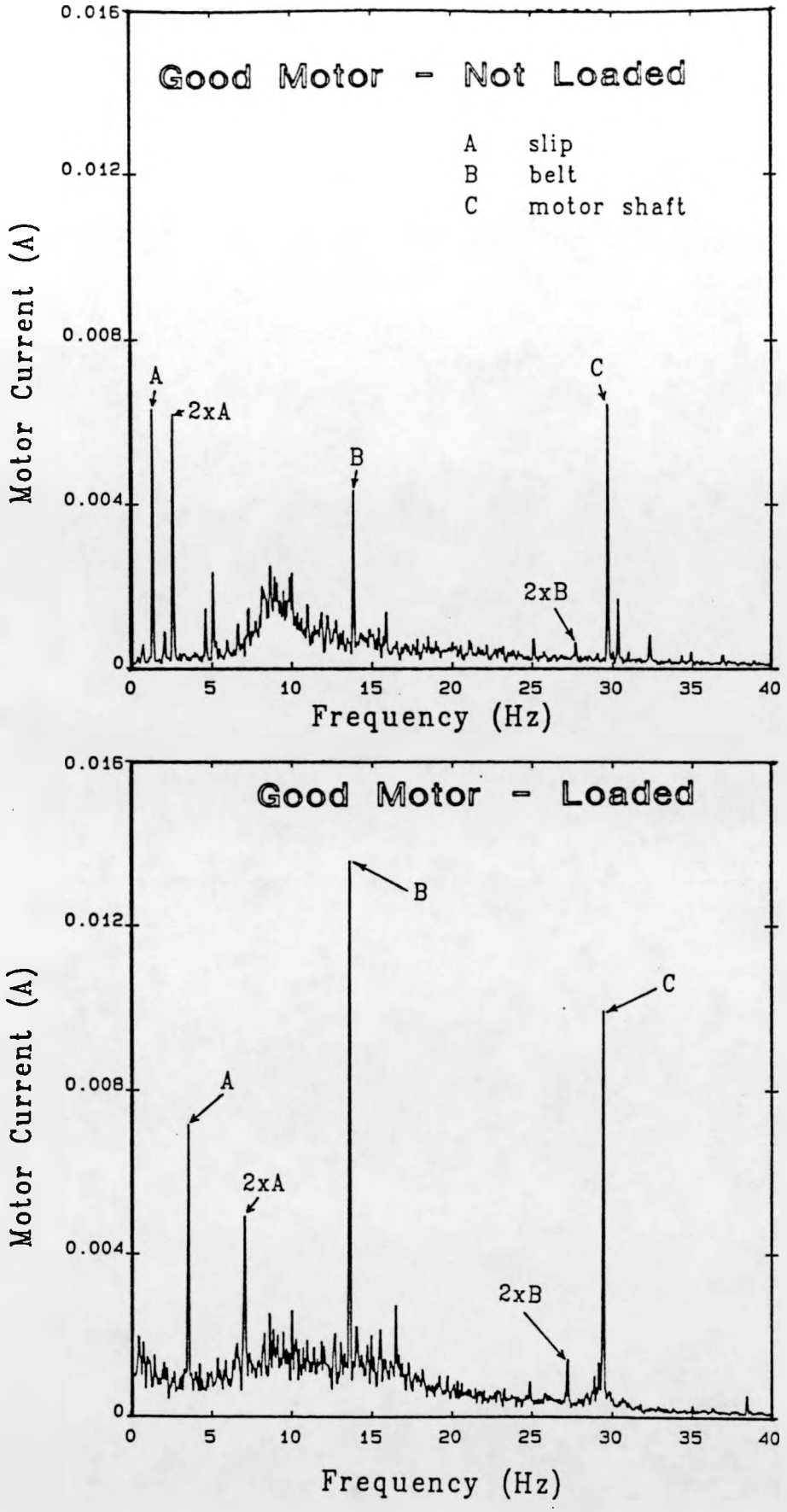

Fig. 20 Demodulated motor current spectra for the good motor of the test rig, operating under no load and while fully loaded by an electric generator.

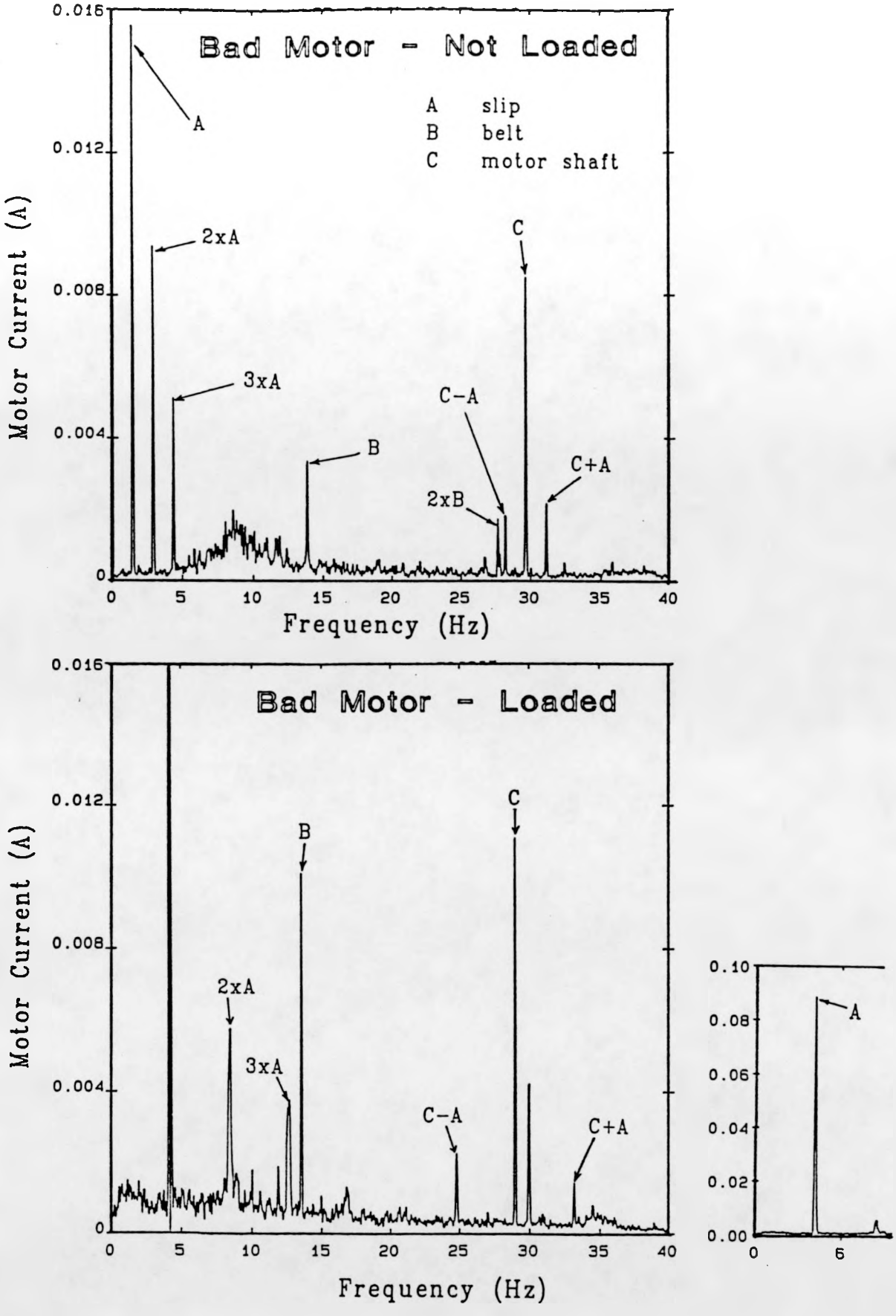

Fig. 21 Demodulated motor current spectra for the faulty motor, under unloaded and loaded conditions.

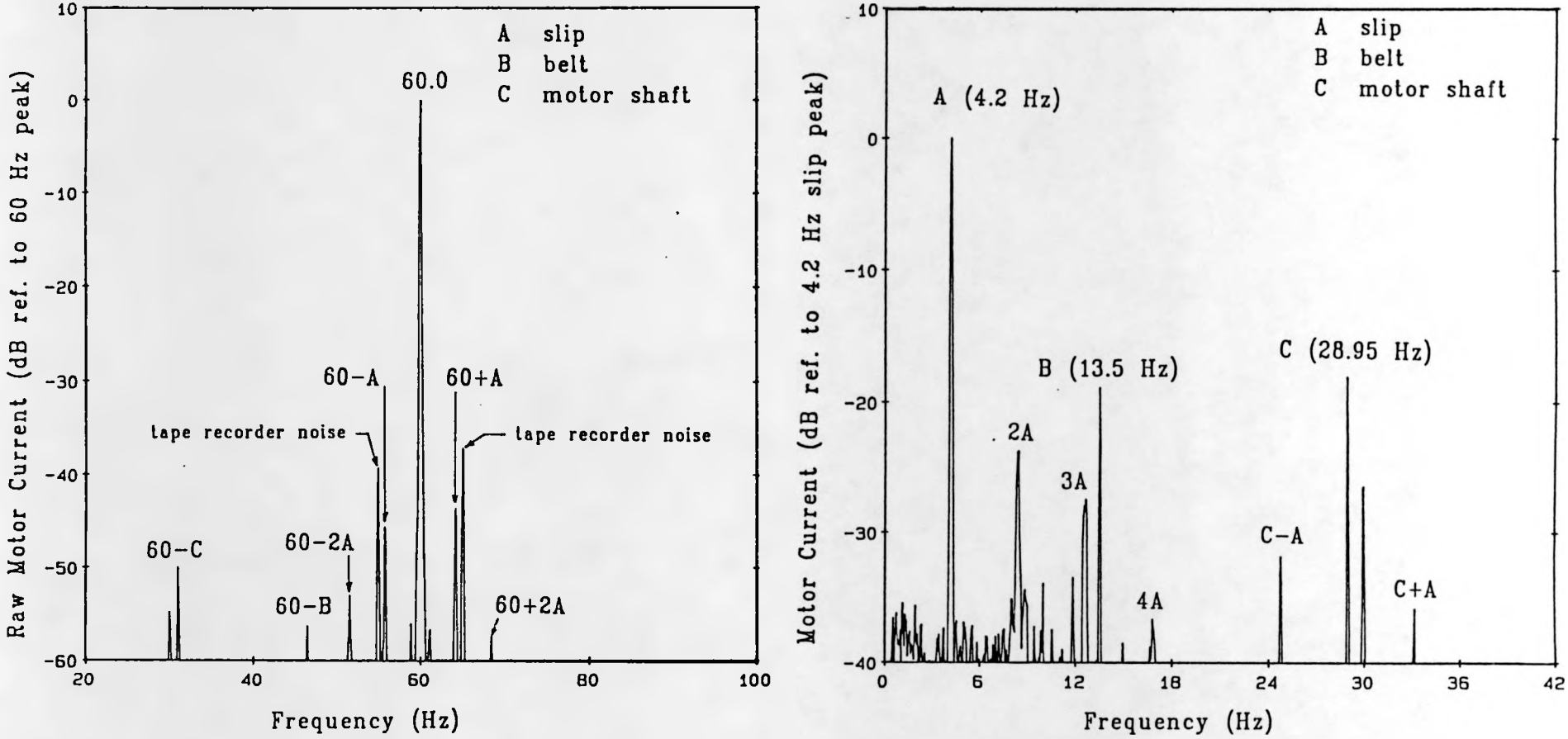

Fig. 22 Spectra of undemodulated (raw) and demodulated motor current signals from the faulty motor of the test rig operating under load.